PolSAR Undeveloped Speckle Suppression Using Clutter Decomposition and Dual-domain Filtering

Yexian Ren

Nanjing University of Information Science and Technology

renyexian@foxmail.com

(yexian_ren@nuist.edu.cn)

Speckle Suppression

- An important topic in SAR remote sensing
  - Estimating physical/polarization parameters;
  - Detection, classification and terrain interpretation…

Random fluctuation of speckle leads to centroid aliasing of different scattering mechanisms

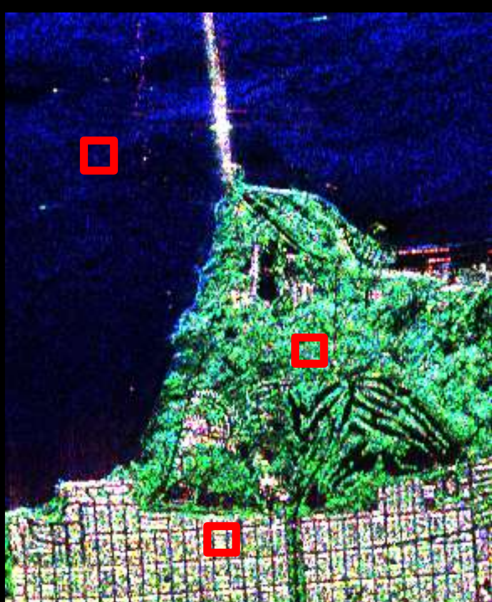

AIRSAR L-band
San Francisco

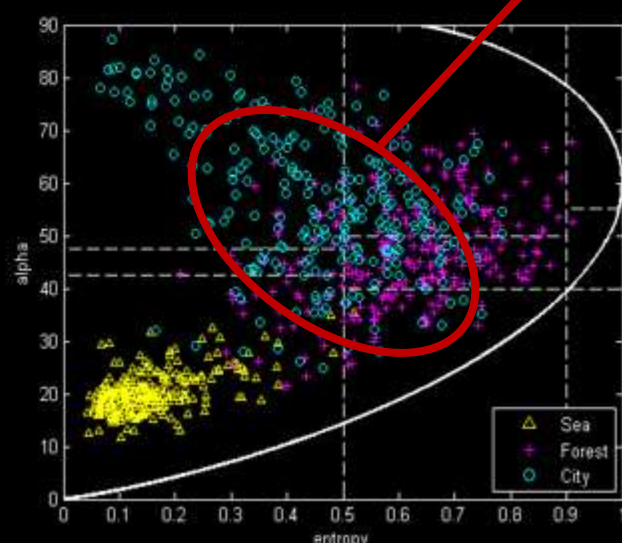

Original 4-look PolSAR image

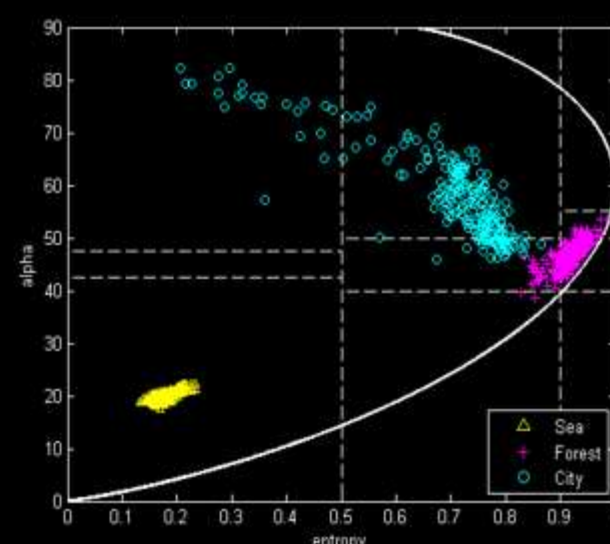

After 7*7 Refined Lee filter

Related Work

- PolSAR speckle filter
  - Nonlocal [Chen et al. 2011, Deledalle et al. 2015]
  - Meanshift [Lang et al. 2014]
  - Adaptive size window [Lang et al. 2015]
  - Extended Sigma [Lee et al. 2016]
  - POSSC [Xu et al. 2016]
  - CV-deSpeckNet [Mullissa et al. 2022]
  - RIRSN [Lin et al. 2023]
  - SDAN [Vasile et al. 2010]
  - ACM [Yang et al. 2016]
  - GMM [Wang et al. 2017]
  - ......

Developed speckle assumption

Undeveloped speckle assumption

Resolution: Medium/low VS High

- HR inevitably leads to heterogeneous clutter

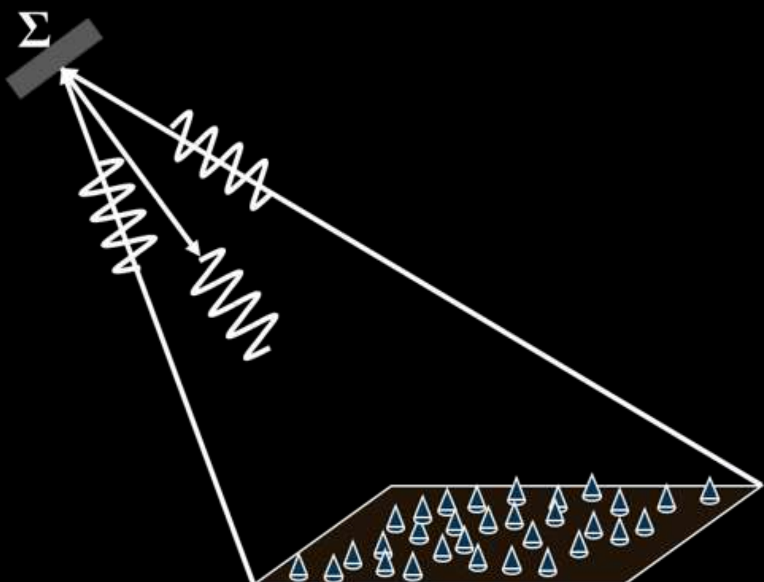

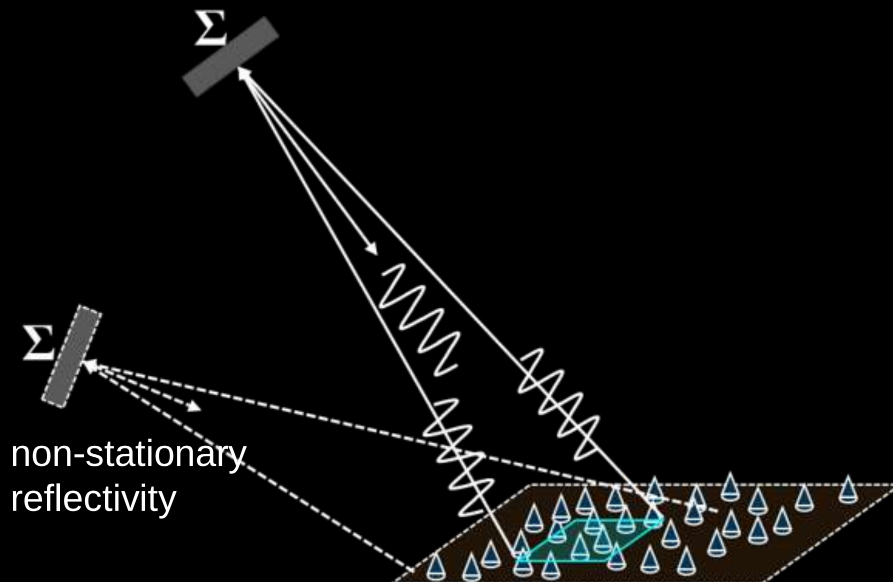

Central limit theorem (CLT)

➡ SLC Gaussian Vectors

➡ Rayleigh, Wishart…

CLT: Insufficient

➡ SLC non-Gaussian Vectors

➡ Heterogeneous clutter

An Interesting Viewpoint about Heterogeneous Sea Clutter

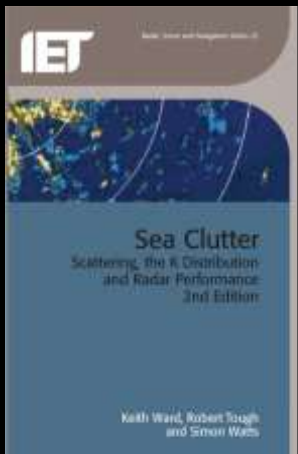

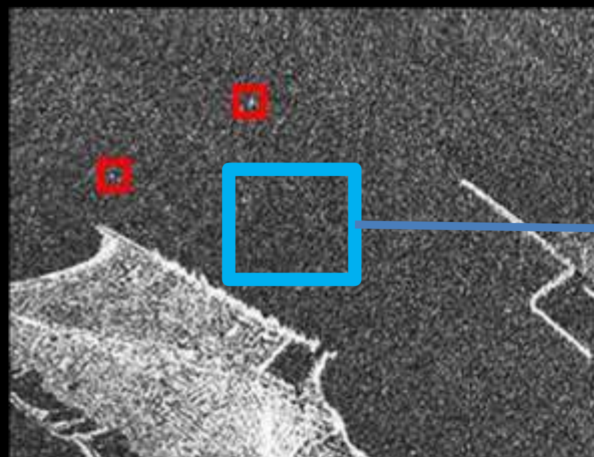

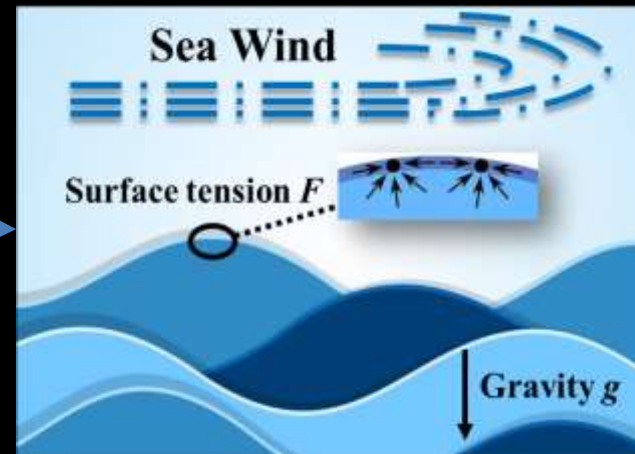

- Sea surface waves can be decomposed into **dual** parts:
  - Surface tension wave
    - *micro scale*, fast-changing (millisecond order), i.e. *speckle*.
  - Gravity wave
    - *macro scale*, slow-changing (second order), i. e. *texture*/modulation.
- Heterogeneous sea clutter is amplitude modulation of tension wave signal by gravity wave signal.

Understanding of HR PolSAR Image

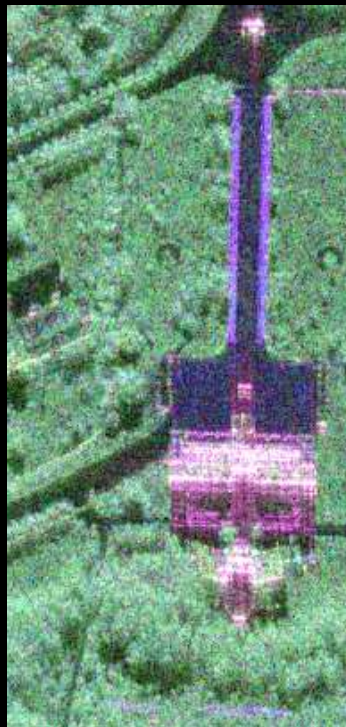

Complex Scattering Vectors

=

Texture
(RCS)

×

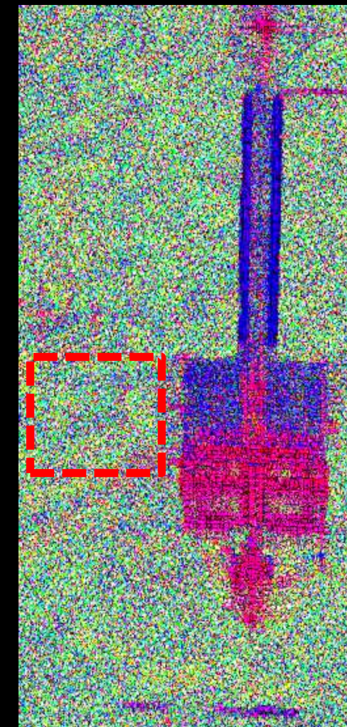

Complex Random Vectors
(Speckle)

$$\mathbf{k} = \sqrt{\tau}\mathbf{z}$$

Texture

Assumptions

- Sparse (visual-pleasing)
- Smooth (slow-changing)

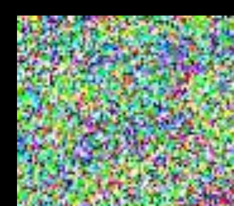

Normalized Vectors

Assumptions

- Gaussian (easy to solve)
- Depolarization (relatively high)

SIRV Model

$$p(\mathbf{k}) = \int_0^{+\infty} \frac{1}{(\pi\tau)^m|\mathbf{M}|}\exp(-\frac{\mathbf{k}^H\mathbf{M}^{-1}\mathbf{k}}{\tau}) \times p(\tau)d\tau$$

Gaussian Term

(Necessary conditions for solving inverse problems)

Non-Gaussian Term

- $\mathbf{M}$: Second-order statistics of speckle
  - Complex correlation between channels
- τ: Non-negative scalar
  - Diverse and uncertain distributions

Likelihood

$$L(\mathbf{k}_1, \mathbf{k}_2, \cdots, \mathbf{k}_N; \mathbf{M}) = \prod_{i=1}^{N} p(\mathbf{k}_i; \mathbf{M})$$

$$= \prod_{i=1}^{N} \int_0^{+\infty} \frac{1}{(\pi\tau)^{\mathrm{m}}|\mathbf{M}|}\exp(-\frac{\mathbf{k}_i^{\mathrm{H}}\mathbf{M}^{-1}\mathbf{k}_i}{\tau}) \times p(\tau)\mathrm{d}\tau$$

τ – M Iteration

- Fix $\mathbf{M}$, update τ:
  - Likelihood

$$\ln L(\mathbf{k}_1, \mathbf{k}_2, \cdots, \mathbf{k}_N; \tau_i|\mathbf{M}) = -N \cdot \ln|\mathbf{M}| - m\sum_{i=1}^{N}\ln(\pi\tau_i) - \sum_{i=1}^{N}\frac{\mathbf{k}_i^H\mathbf{M}^{-1}\mathbf{k}_i}{\tau_i}$$

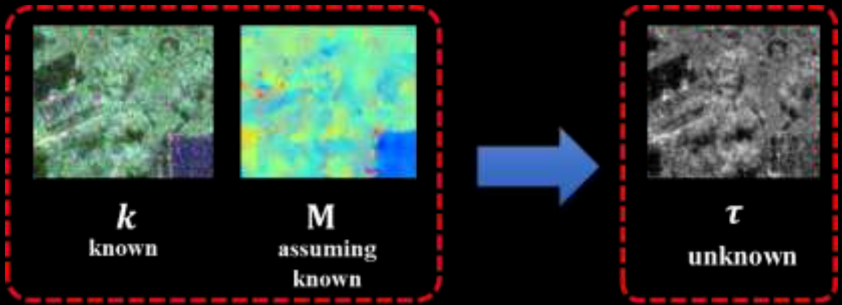

  - Estimation

$$\frac{\partial \ln L(\mathbf{k}_1, \mathbf{k}_2, \cdots, \mathbf{k}_N; \tau_i|\mathbf{M})}{\partial \tau_i} = 0 \Rightarrow -m\sum_{i=1}^{N}\frac{1}{\tau_i} + \sum_{i=1}^{N}\frac{\mathbf{k}_i^H\mathbf{M}^{-1}\mathbf{k}_i}{\tau_i^2} = 0$$

$$\Rightarrow \hat{\tau}_i = \frac{\mathbf{k}_i^H\mathbf{M}^{-1}\mathbf{k}_i}{m}$$

$\tau - \mathbf{M}$ Iteration

- Fix τ, update $\mathbf{M}$:
  - Likelihood

$$\ln L(\mathbf{k}_1, \mathbf{k}_2, \cdots, \mathbf{k}_N; \mathbf{M}|\tau_1, \tau_2, \cdots, \tau_N) = -N \cdot \ln|\mathbf{M}| - m \sum_{i=1}^{N} \ln(\pi\tau_i) - \sum_{i=1}^{N} \frac{\mathbf{k}_i^H \mathbf{M}^{-1} \mathbf{k}_i}{\tau_i}$$

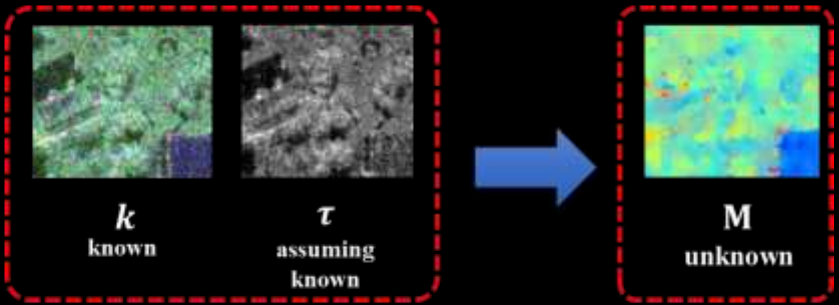

  - Estimation

$$\frac{\partial \ln L(\mathbf{k}_1, \mathbf{k}_2, \cdots, \mathbf{k}_N; \mathbf{M}|\tau_1, \tau_2, \cdots, \tau_N)}{\partial \mathbf{M}} = 0 \Rightarrow -N \cdot \mathbf{M}^{-1} - \sum_{i=1}^{N} \frac{-\mathbf{k}_i \mathbf{k}_i^H \mathbf{M}^{-2}}{\tau_i} = 0$$

$$\Rightarrow \widehat{\mathbf{M}} = \frac{1}{N} \sum_{i=1}^{N} \frac{\mathbf{k}_i \mathbf{k}_i^H}{\tau_i}$$

$\tau - \mathbf{M}$ Iteration

- Fixed point iteration (SIRV estimator)

$$\widehat{\mathbf{M}}(j+1) = \frac{m}{N}\sum_{i=1}^{N}\frac{\mathbf{k}_i\mathbf{k}_i^H}{\mathbf{k}_i^H\widehat{\mathbf{M}}^{-1}(j)\mathbf{k}_i}$$

Generalization

L-look case: $\mathbf{T}$

$$\widehat{\mathbf{M}}(j+1) = \frac{m}{N}\sum_{i=1}^{N}\frac{\mathbf{T}_i}{\mathrm{Tr}\left(\widehat{\mathbf{M}}^{-1}(j)\mathbf{T}_i\right)}$$

- Iteration initialization

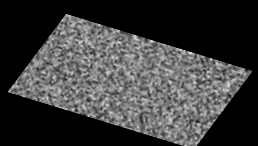

near

far

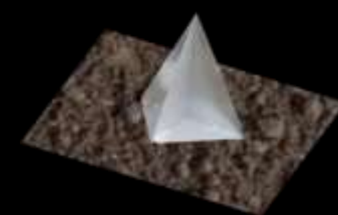

white noise

$(Entropy = 1)$

$$\mathbf{M} \approx \begin{bmatrix}1 & 0 & 0\\ 0 & 1 & 0\\ 0 & 0 & 1\end{bmatrix}$$

completely decoherence

start

speckle

$\approx$ colored-noise

$(0 < Entropy < 1)$

$\mathbf{M}$

partial decoherence

Example

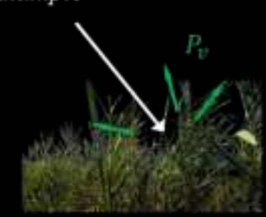

volume ≠ white noise

$$\frac{1}{4}\begin{bmatrix}2 & 0 & 0\\ 0 & 1 & 0\\ 0 & 0 & 1\end{bmatrix} \quad \frac{1}{30}\begin{bmatrix}15 & \pm5 & 0\\ \pm5 & 7 & 0\\ 0 & 0 & 8\end{bmatrix}$$

point target

$(Entropy \rightarrow 0)$

$$\mathbf{M} \approx \begin{bmatrix}1 & \beta^* & 0\\ \beta & |\beta|^2 & 0\\ 0 & 0 & 0\end{bmatrix}$$

almost completely coherent

not full rank

Clutter Decomposition Problem

- Using original SIRV estimator
  - Showing poor performance

Problem is not solved

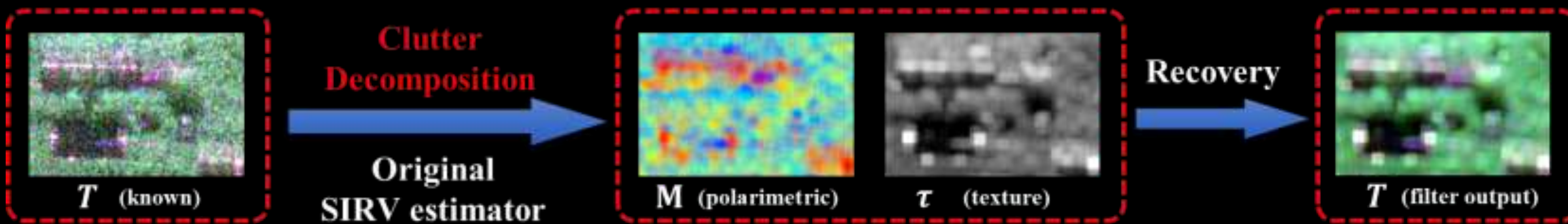

- Using dual-domain filter
  - Showing technical superiority

Problem is largely solved

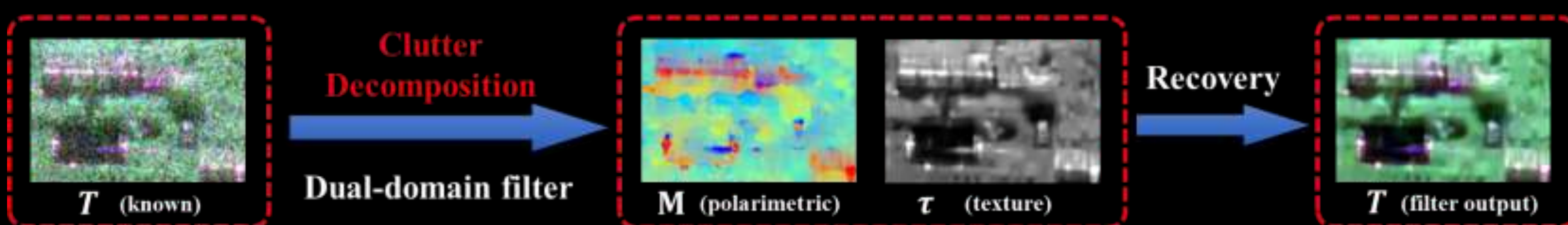

Clutter Decomposition and Dual-domain Filtering

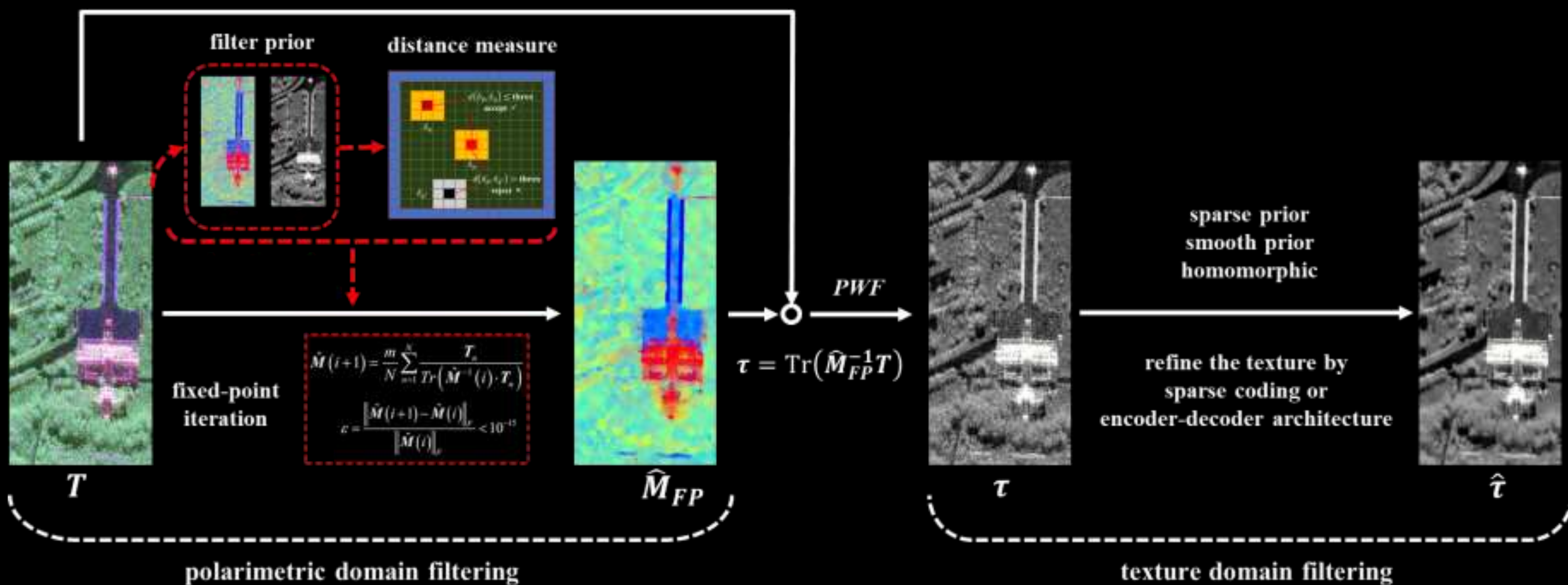

- Use multilook-like operation
- Preserve HR polarimetric information

- Use flexible operation in CV
- Enhance visual effect

Polarimetric Domain Filtering

Using rough estimation as filter prior for refined estimation

Screen similar samples for matrix estimation

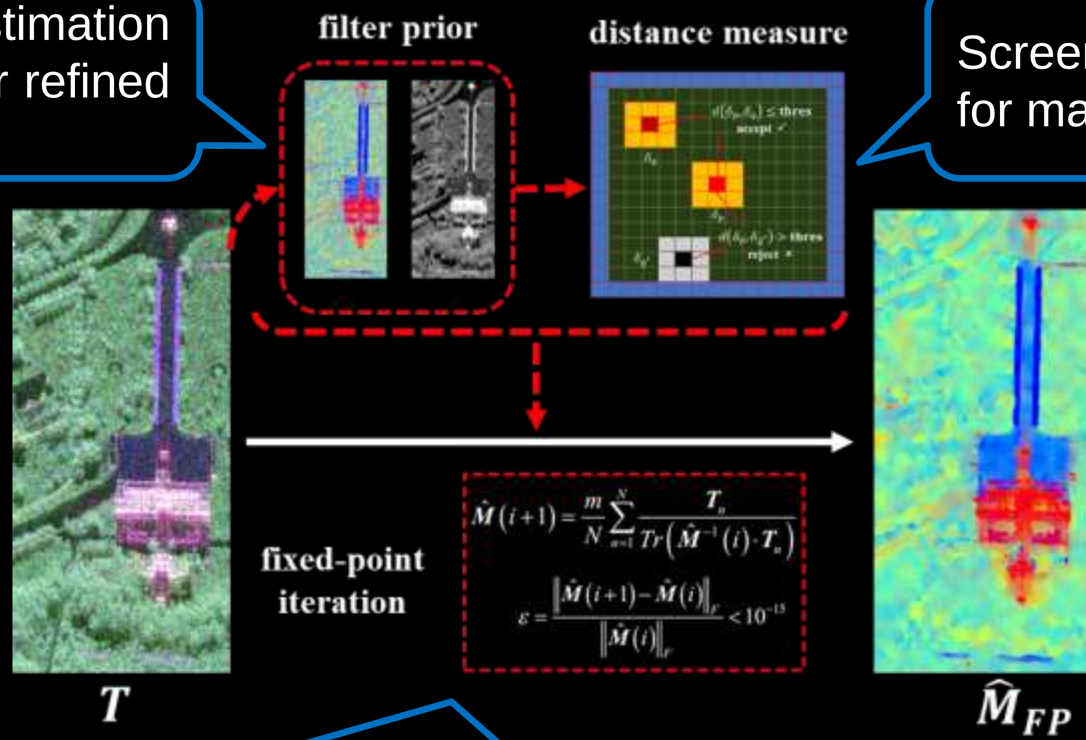

Eliminating data scale/level caused by texture fluctuations in **Coherency Estimation**.

Remark: Each iteration strictly obeys Lee's three filtering principles to preserve polarimetric scattering information, especially consistency of correlation and phase difference.

Texture Domain Filtering

PWF：key connection between two filters

- separate polarimetric information
- **speckle decorrelation** (meaningless pure noise)
- improve SCR without loss of resolution (2.7 dB gain)

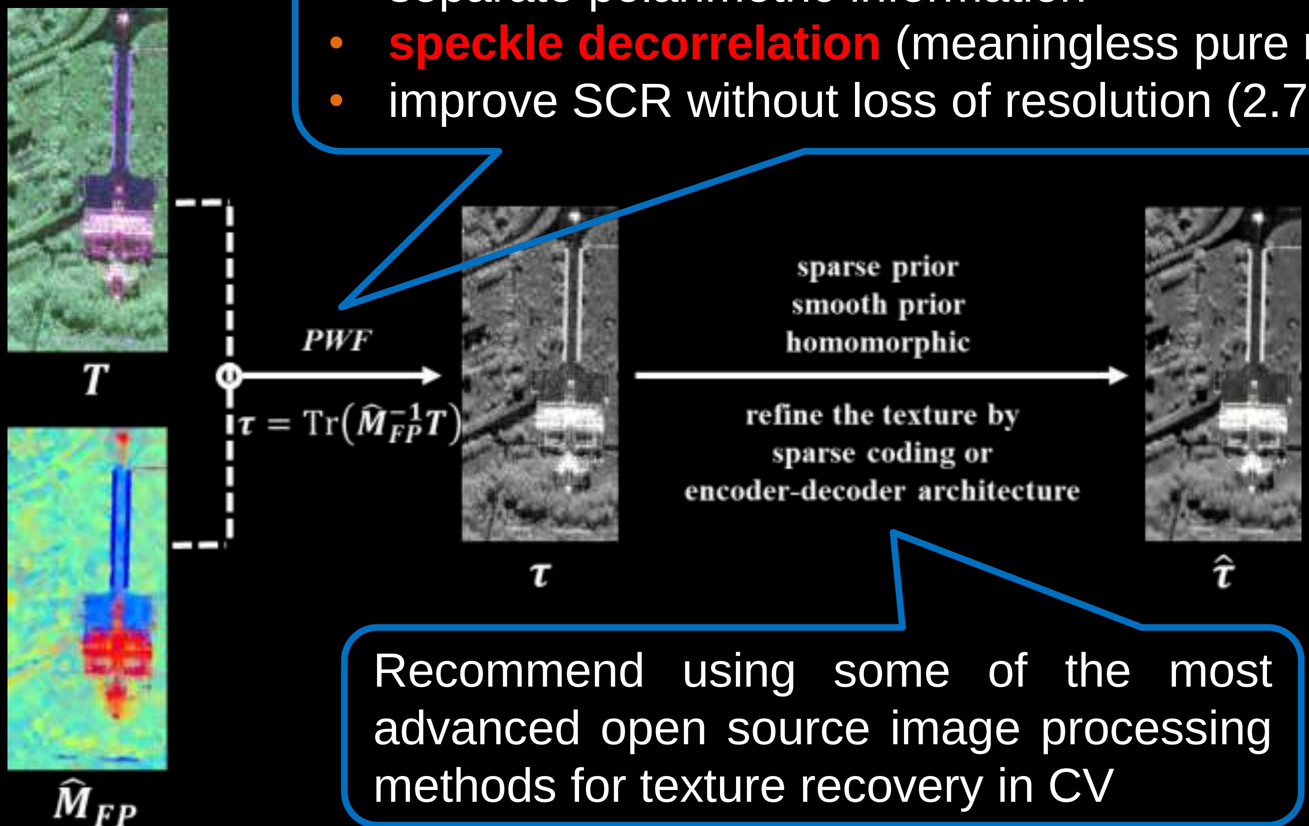

Recommend using some of the most advanced open source image processing methods for texture recovery in CV

Remark: SOTA methods in CV can be flexibly applied for texture image processing, including sparse coding and NN-based encoder -decoder methods.

Dual-domain Fusion

- HR PolSAR recovery is an image fussion problem

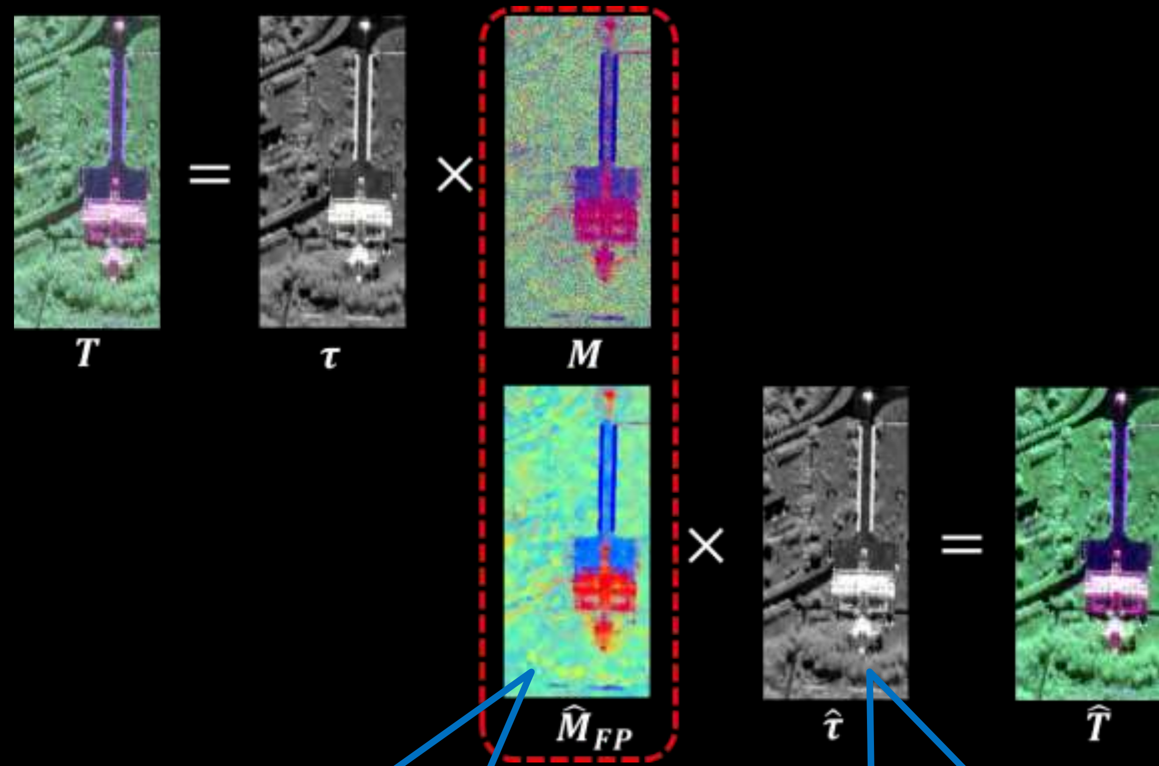

polarimetric information
relatively low resolution

semantic information
relatively high resolution

Mixed Distance Measure

- Integrating texture and polarization information

$$d_m = \frac{1}{K}\sum_{k}^{K}\left[(1-\alpha)\left[\frac{1}{2}\left(\frac{\tilde{\tau}_{\delta_p(k)}}{\tilde{\tau}_{\delta_q(k)}}+\frac{\tilde{\tau}_{\delta_q(k)}}{\tilde{\tau}_{\delta_p(k)}}\right)-1\right]+\alpha\left[1-\frac{\mathrm{Tr}\left(\widetilde{\mathbf{M}}_{\delta_p(k)}\widetilde{\mathbf{M}}_{\delta_q(k)}\right)}{\sqrt{\mathrm{Tr}\left(\widetilde{\mathbf{M}}_{\delta_p(k)}\widetilde{\mathbf{M}}_{\delta_p(k)}\right)\mathrm{Tr}\left(\widetilde{\mathbf{M}}_{\delta_q(k)}\widetilde{\mathbf{M}}_{\delta_q(k)}\right)}}\right]\right]$$

texture info.
multiplicative noise (ratio)

polarimetric info.
no need for full rank
rotation invariant

- Phenomenon: targets with the similar texture but different polarimetric properties
  - the coefficient alpha can be slightly larger than 0.5, such as 0.6
  - $\ln Q$ is greatly affected by power/SPAN values
  - d_m use more information in sample screening

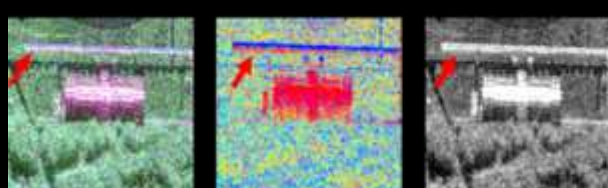

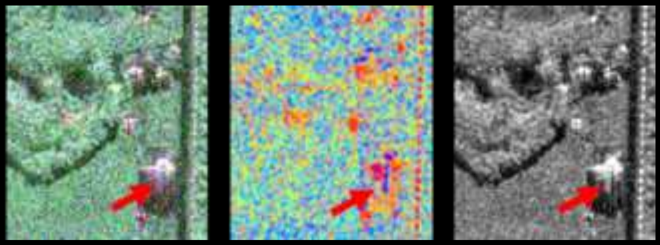

Results: CETC-38 X-PolSAR Data, Hainan Lingshui

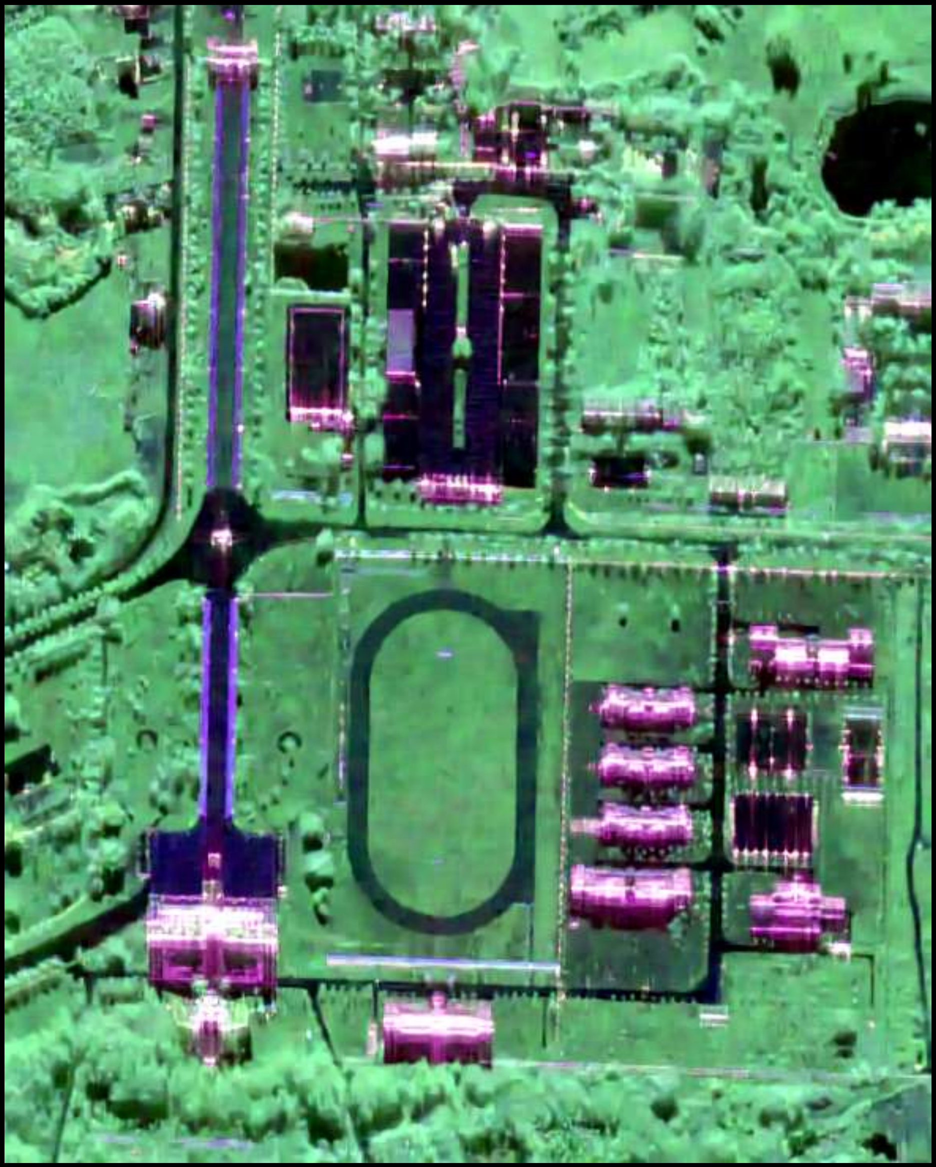

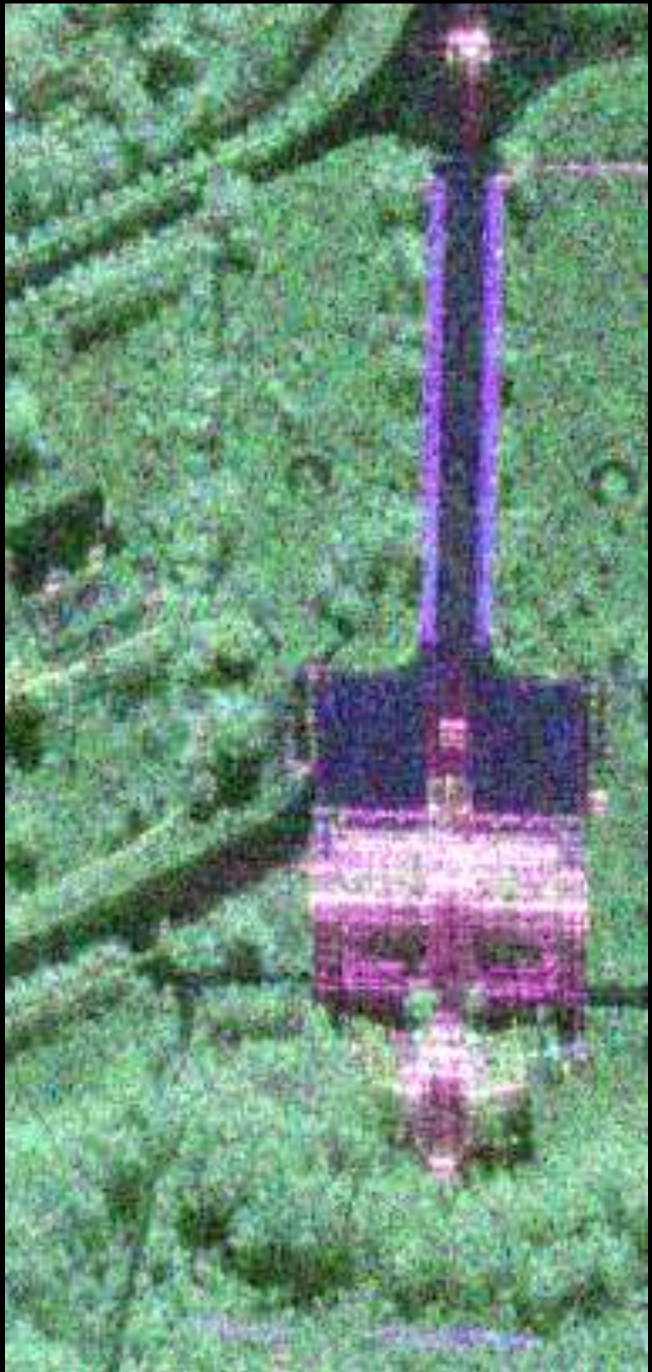

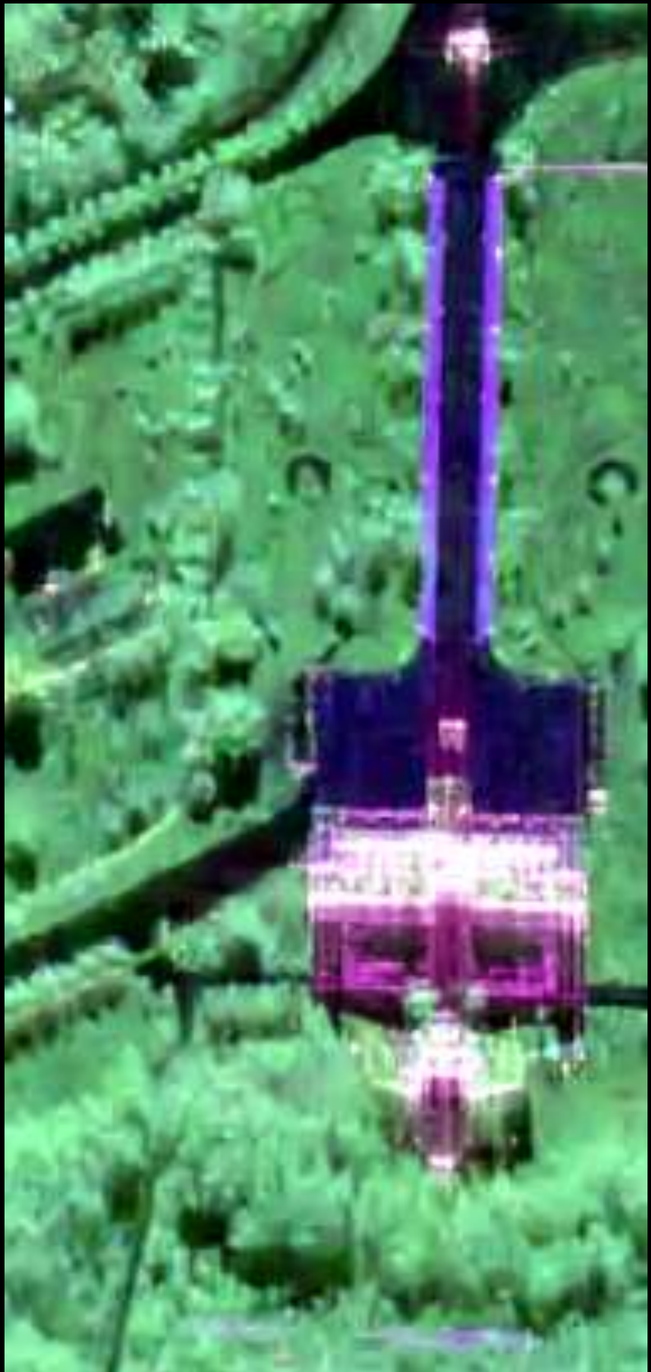

Results: Normalized Coherency Matrix

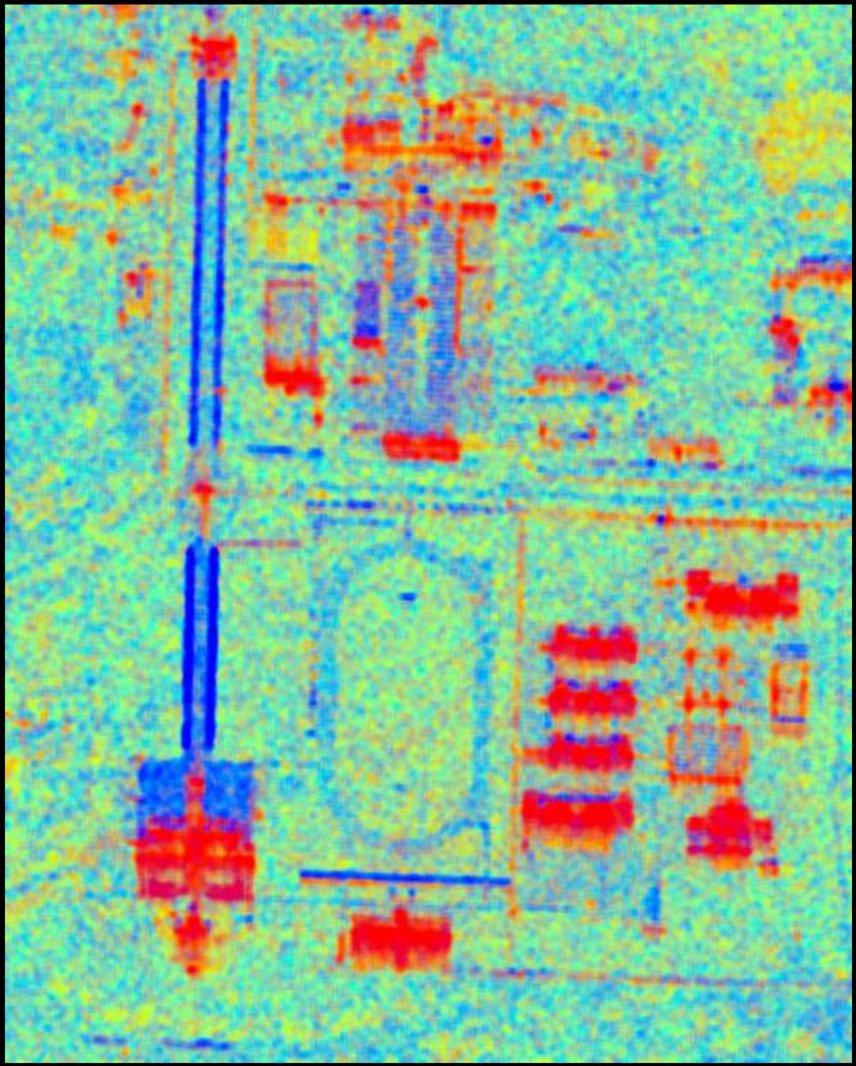

Original 7 × 7 SIRV estimator

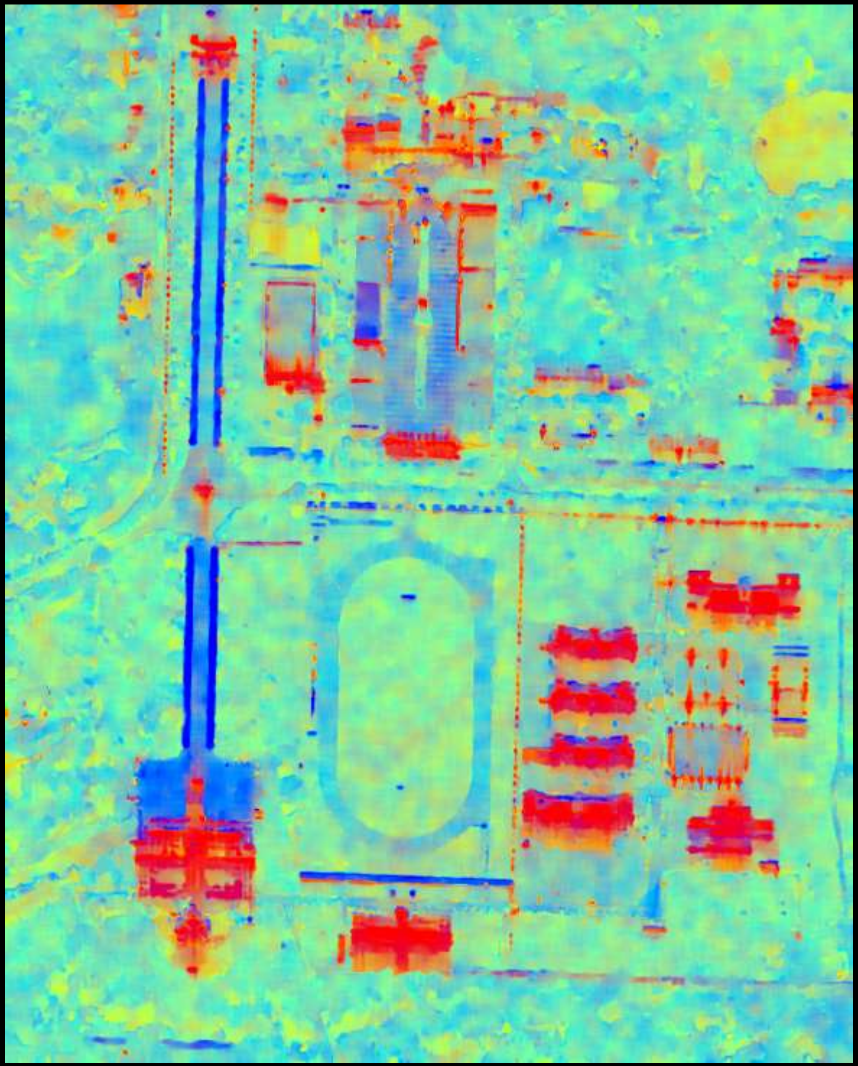

Dual-domain filter result

Results: CETC-38 X-PolSAR Data, Hainan Lingshui

Before filtering

After filtering

Results: DLR FSAR S-PolSAR Data, Kaufbeuren


Results: AIRCAS C-PolSAR Data, Hebei Zunhua

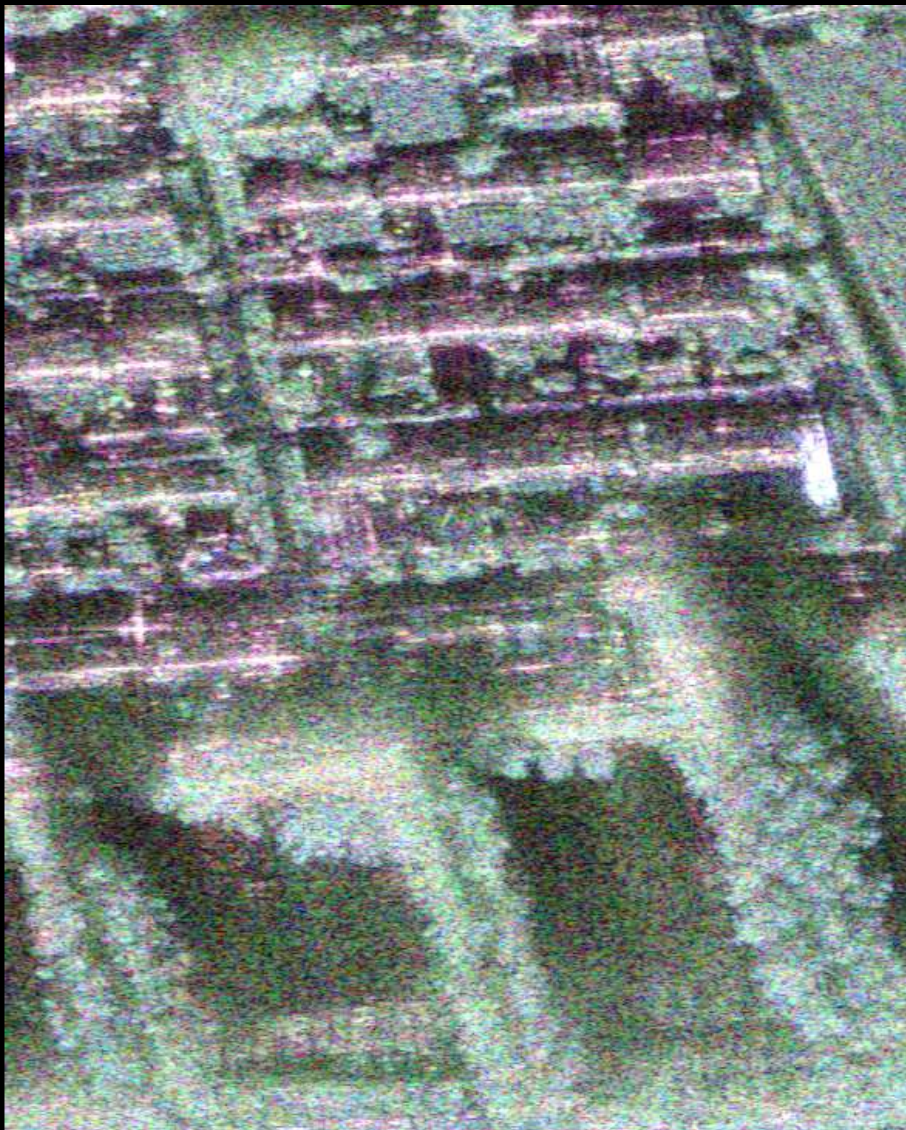

Results: DLR ESAR L-SAR Oberpfaffenhofen

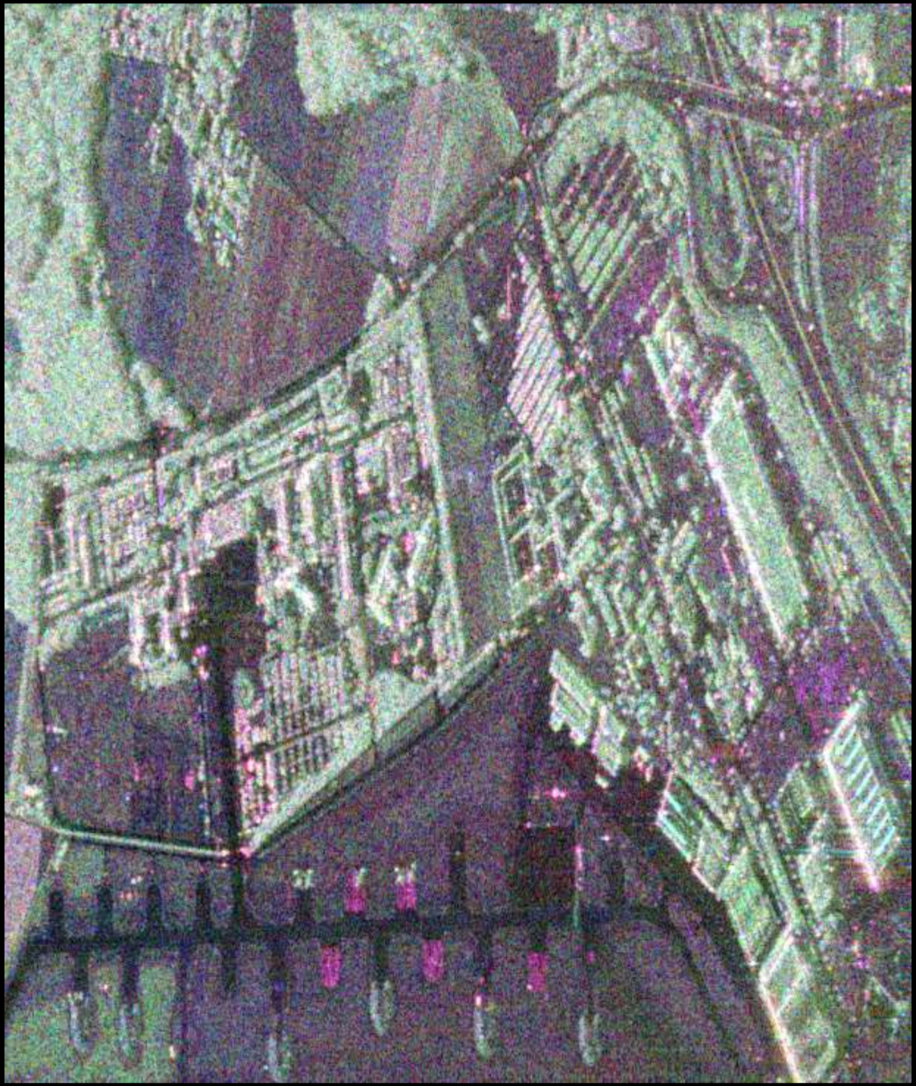

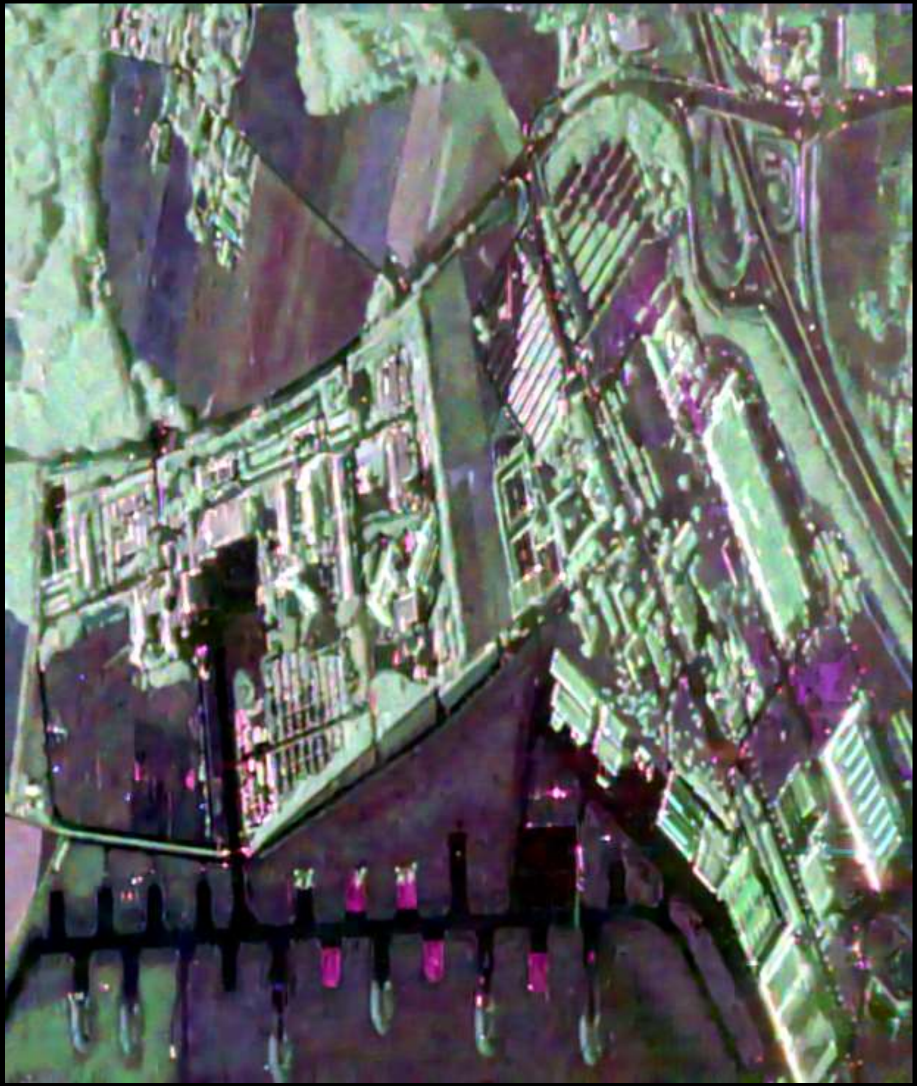

Results: GF-3 Sea Wave Recovery

Results: GF-3 City, Xi An

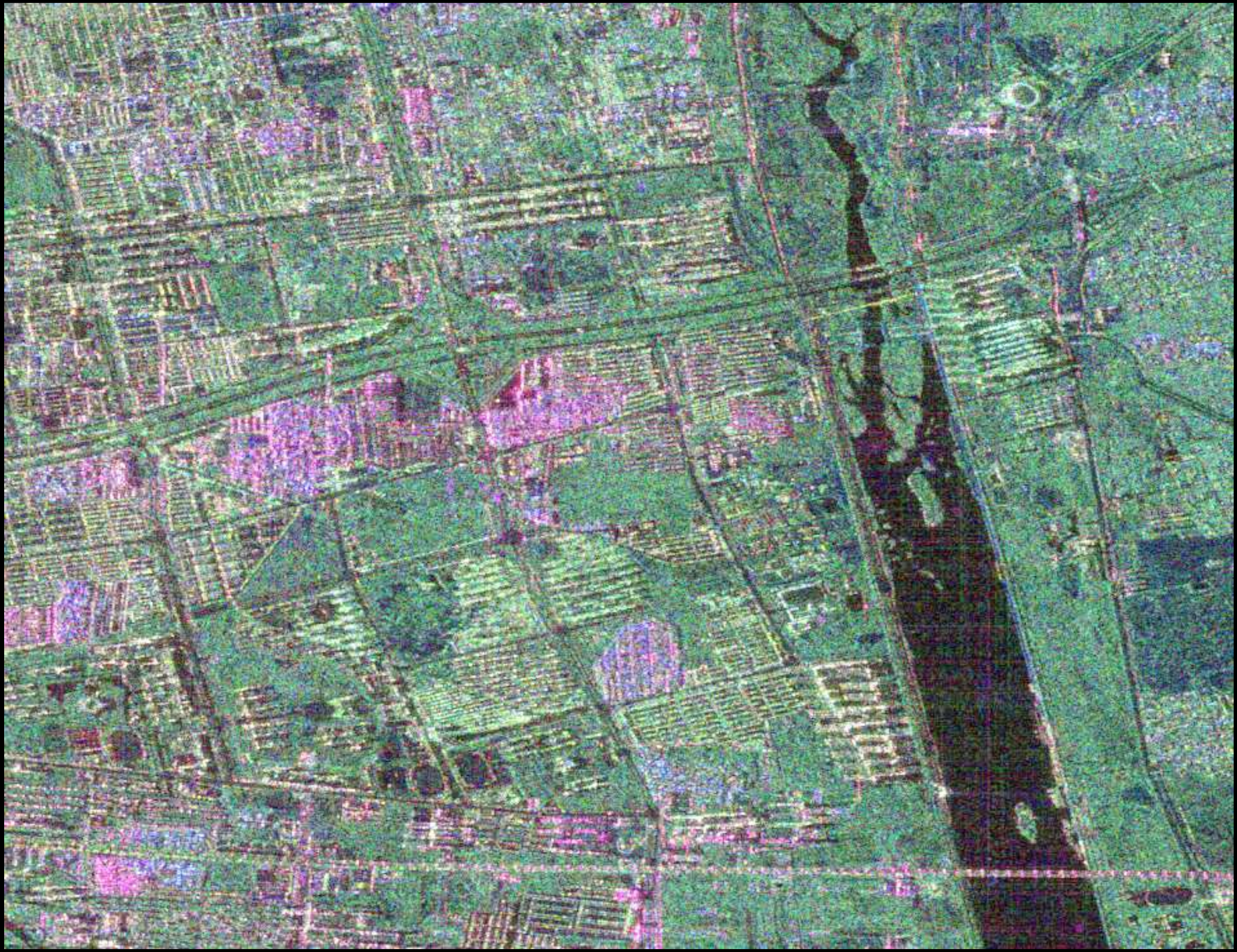

Single Look
Complex

Results: GF-3 City, Xi An

Filtering Result

Comparisons

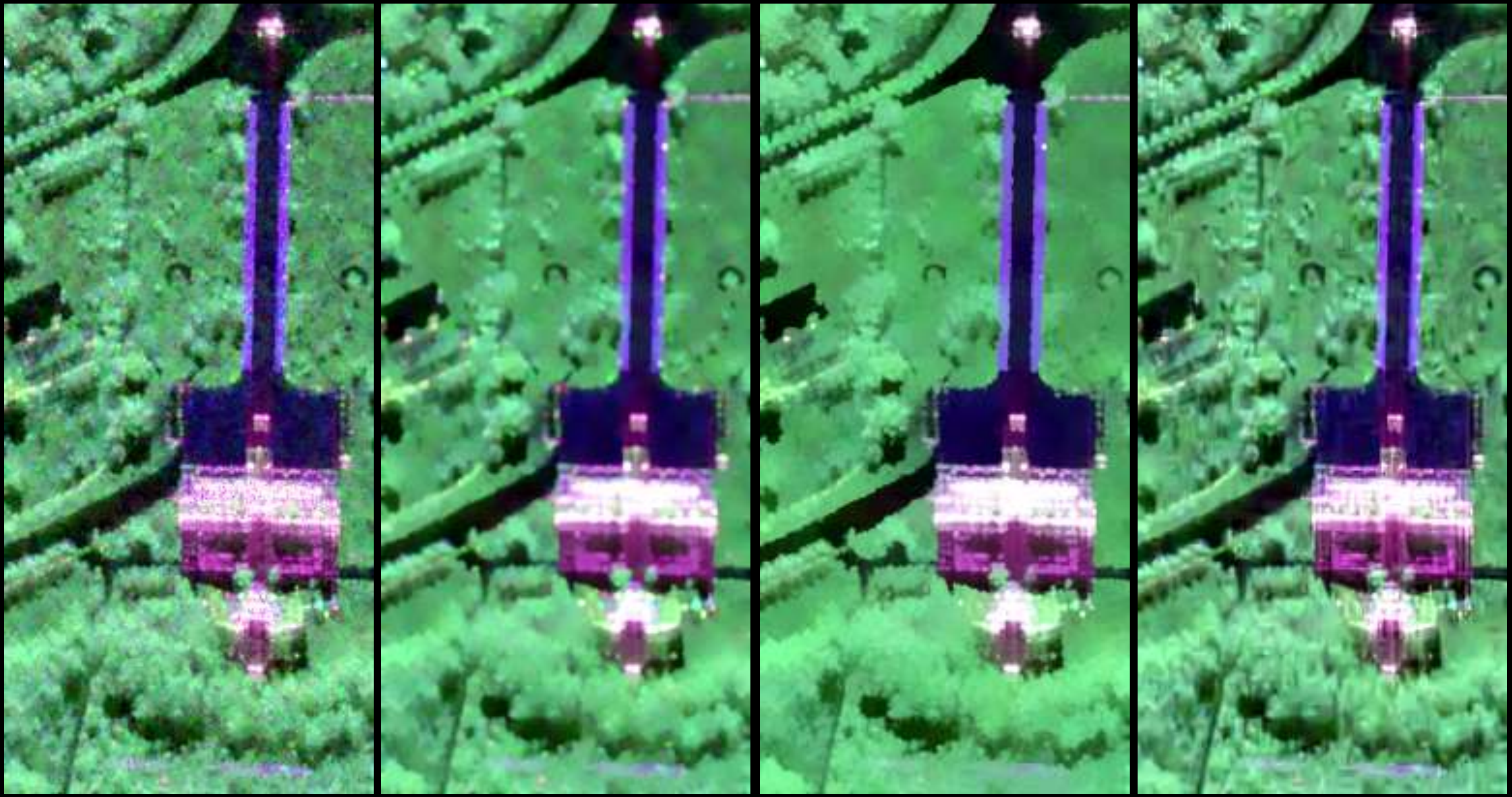

Improved Sigma | **Nonlocal pretest** | **Mean shift** | **Dual-domain**

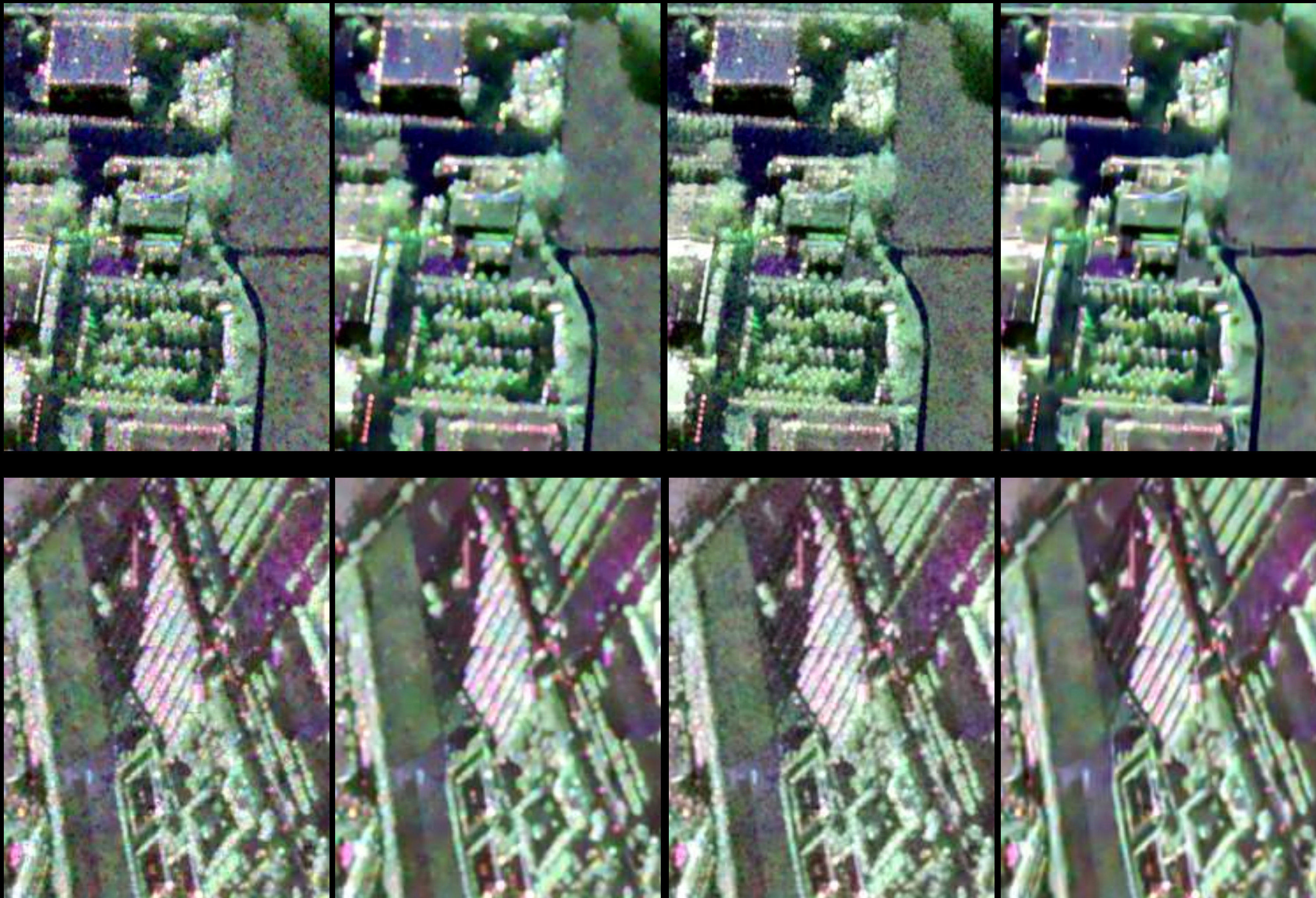

Improved Sigma **Nonlocal pretest** **Mean shift** **Dual-domain**

Separated Multiplicative Noise (Ratio Image)

CETC-38 X-band data	$E_r[T_{11}]$	$E_r[T_{22}]$	$E_r[T_{33}]$	$SD_r[T_{11}]$	$SD_r[T_{22}]$	$SD_r[T_{33}]$
Improved sigma	0.8702	0.8719	0.8802	0.5879	0.5967	0.5983
Nonlocal pretest	0.9006	0.8992	0.9197	0.9174	0.9183	0.9110
Mean shift	0.7846	0.7843	0.8058	0.9403	0.9824	0.9603
Dual-domain filter	**0.9906**	**0.9913**	**0.9909**	**1.0020**	**1.0094**	**0.9997**
F-SAR S-band data	$E_r[T_{11}]$	$E_r[T_{22}]$	$E_r[T_{33}]$	$SD_r[T_{11}]$	$SD_r[T_{22}]$	$SD_r[T_{33}]$
Improved sigma	0.8904	0.8928	0.8936	0.5555	0.5630	0.5603
Nonlocal pretest	0.9034	0.8961	0.9041	0.7755	0.7780	0.7731
Mean shift	0.8855	0.8807	0.8752	0.7817	0.7835	0.7327
Dual-domain filter	**1.0031**	**1.0303**	**1.0403**	**0.9344**	**0.9654**	**0.9699**

$$E_r = \frac{1}{N}\sum_{n=1}^{N}\left(\frac{I_0}{I_1}\right)_n, SD_r = \sqrt{\frac{1}{N}\sum_{n=1}^{N}(r_n - 1)^2}$$

- **Calculate on 1000×800 single-look PolSAR image**

Theoretical value: $E_r = 1; SD_r = \sqrt{1/_{look}} = 1$。

If E_r deviates too much from 1, it shows radiation distortion.

If SD_r far less than 1， the speckle suppression is not complete.

If $SD_r$is greater than the theoretical value, the results deviate from the true RCS.

Point Targets Preservation

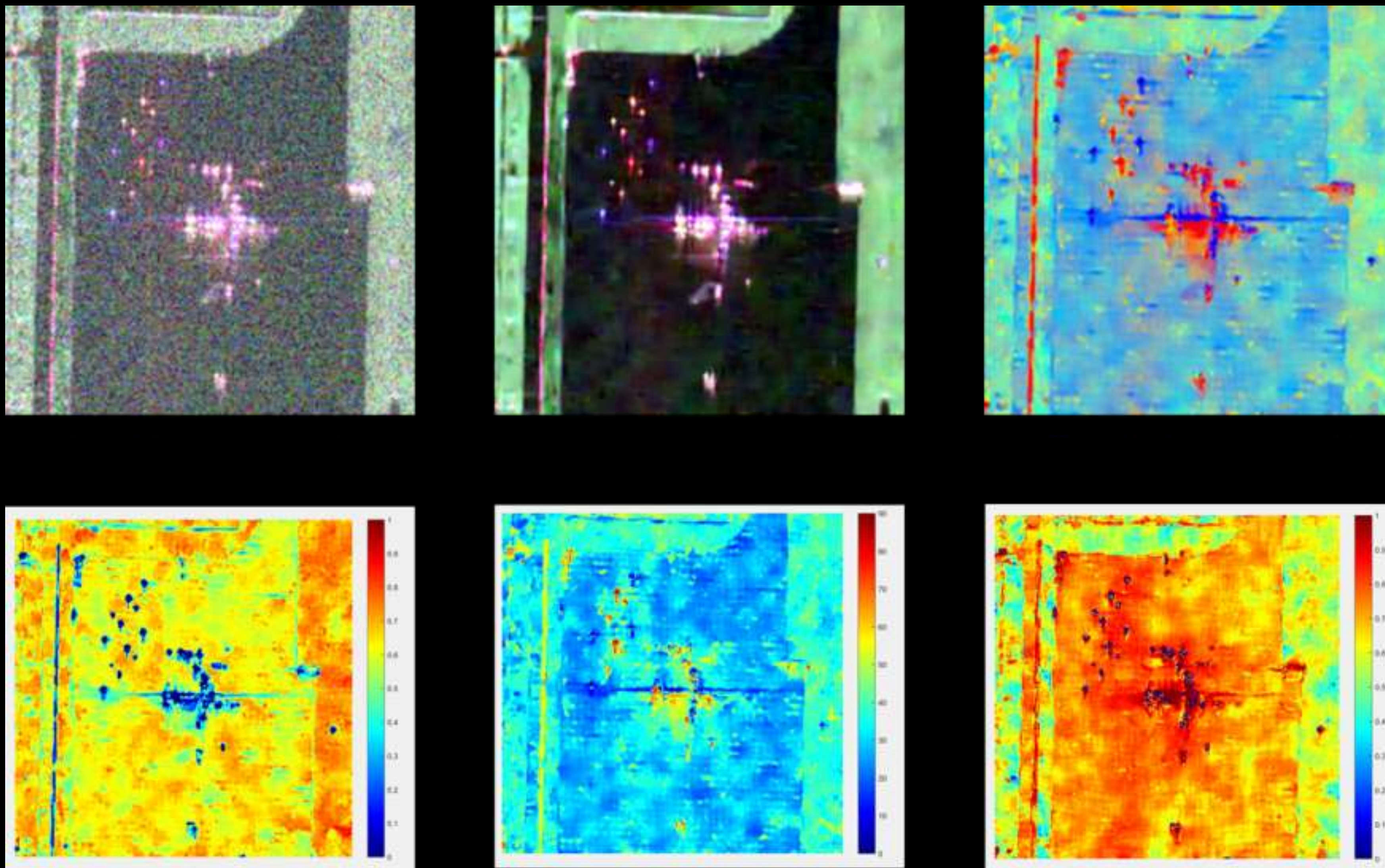

H **Alpha** **A**

Tm-ENL: From 1 to 100

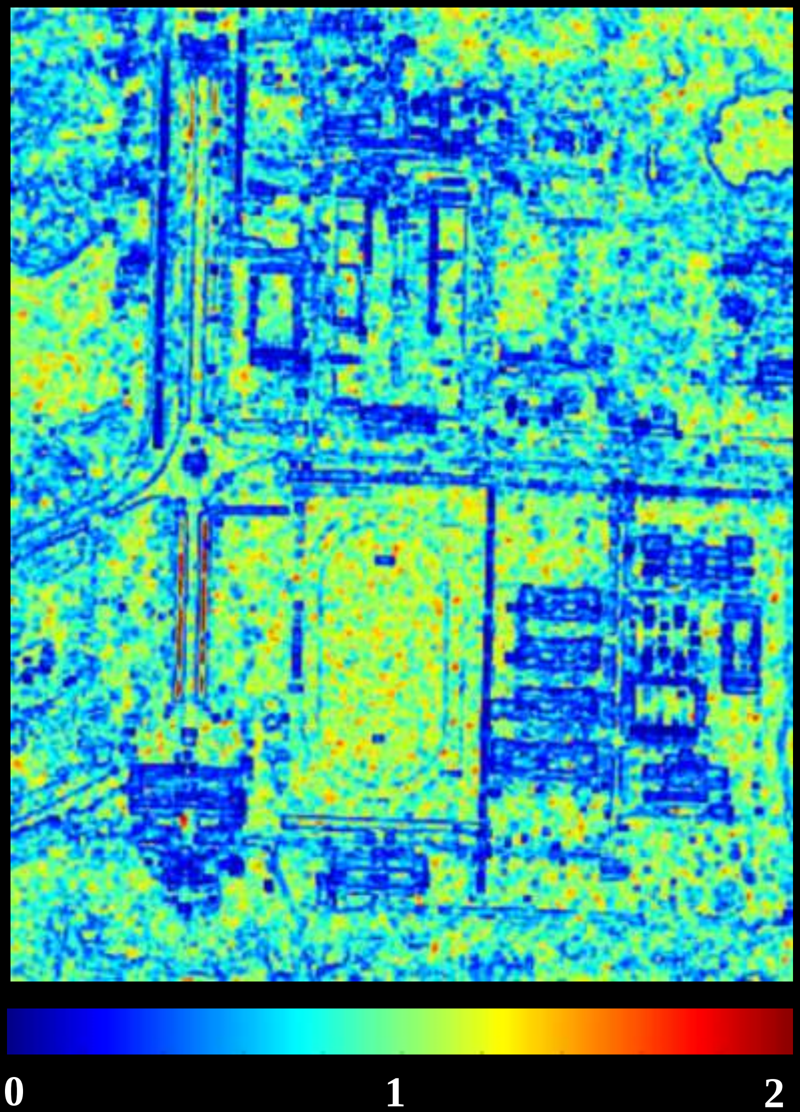

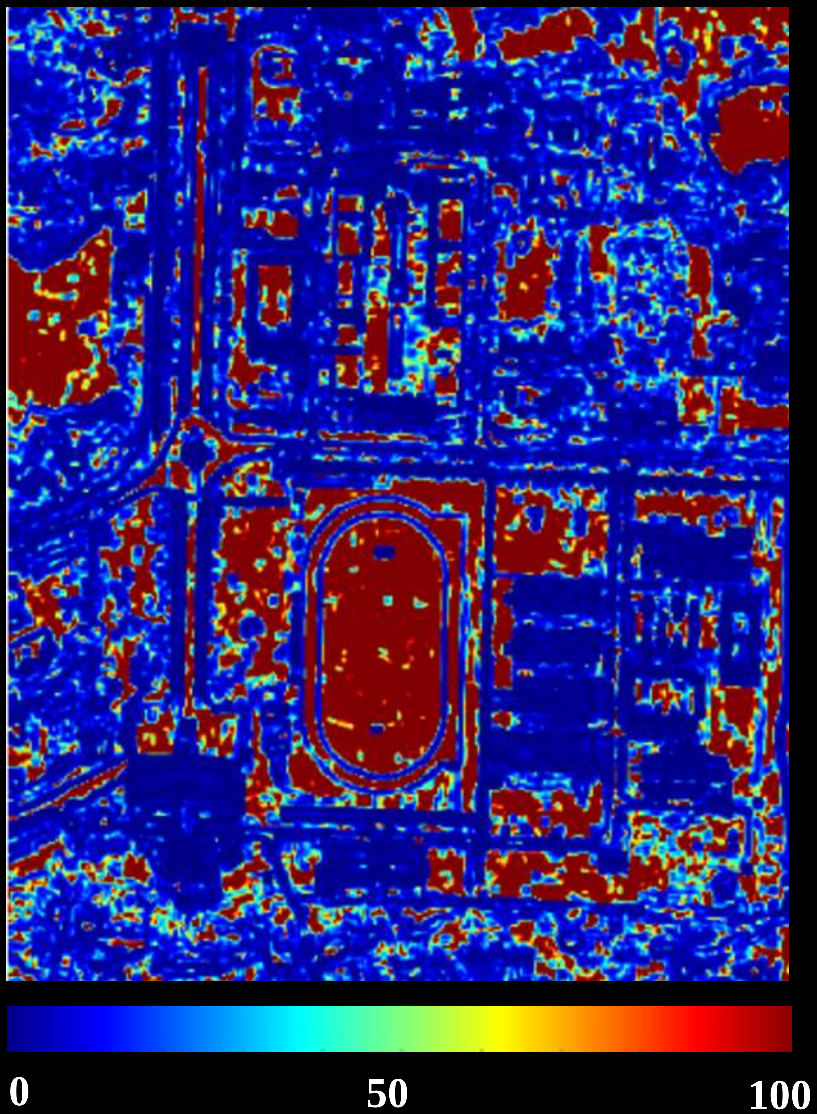

By-product: High-Resolution Heterogeneity

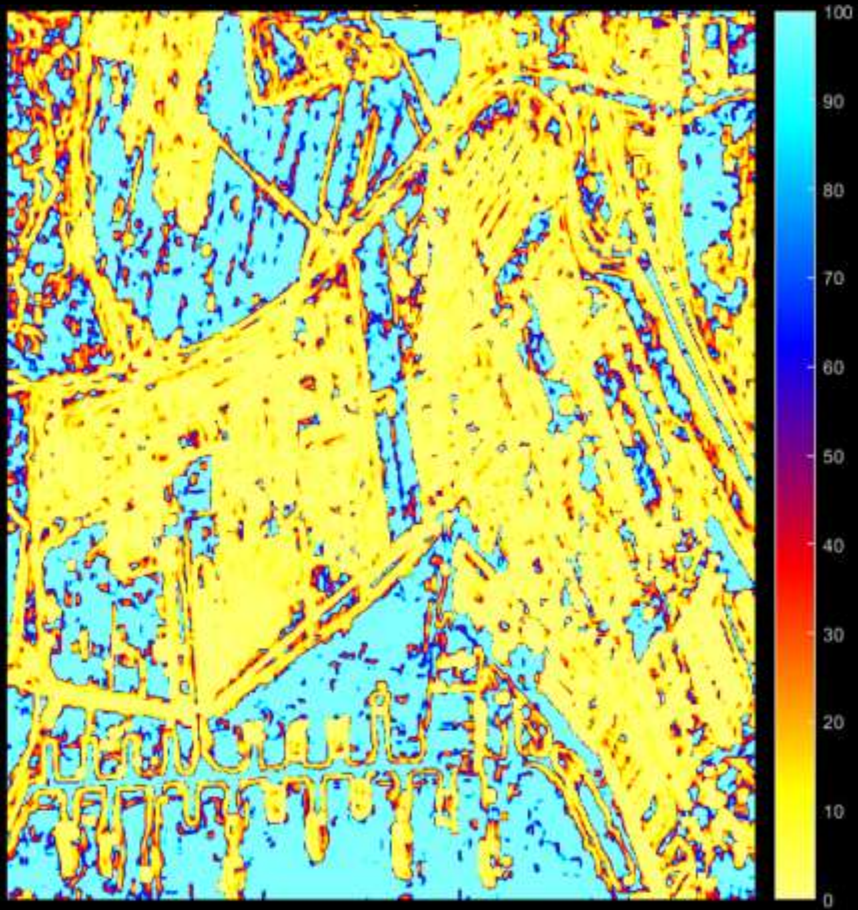

Trace-moment ENL
(Low-Resolution)

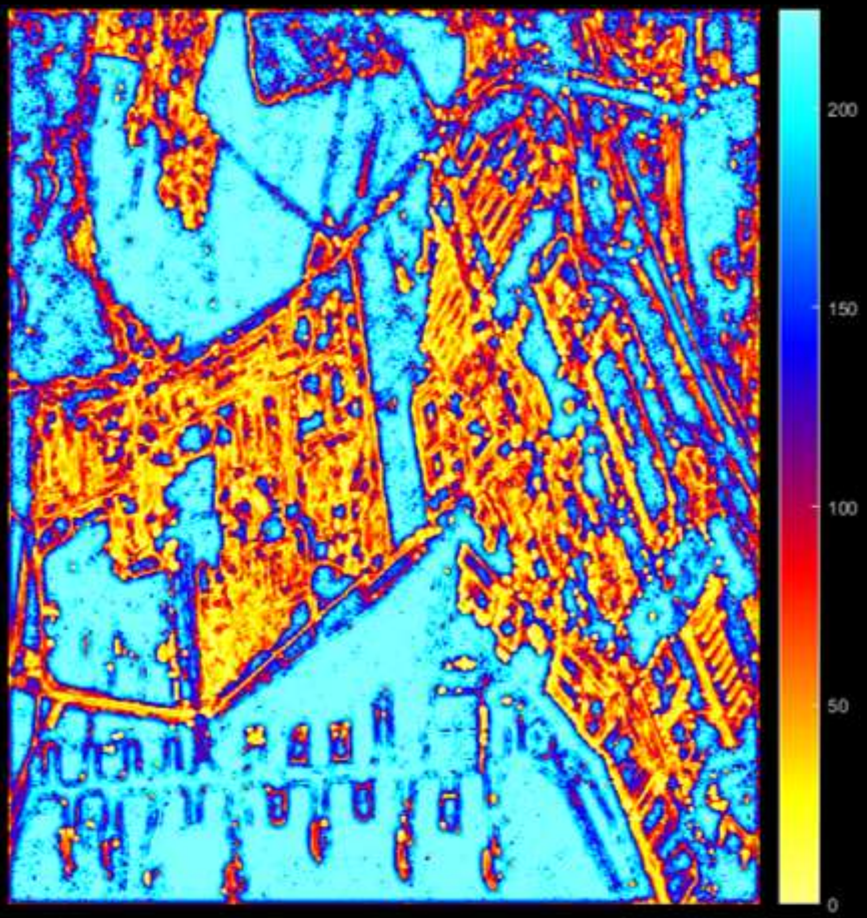

The number of similar samples
(polarimetric domain filtering)

By-product: High-Resolution H/alpha/A

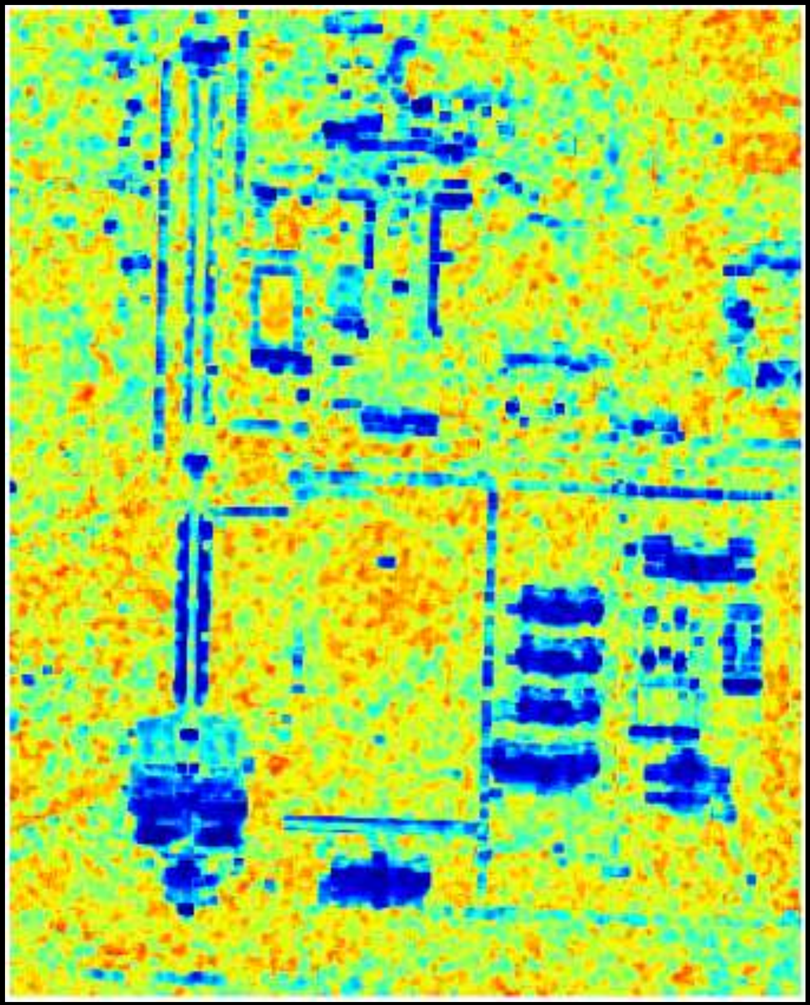

81-look

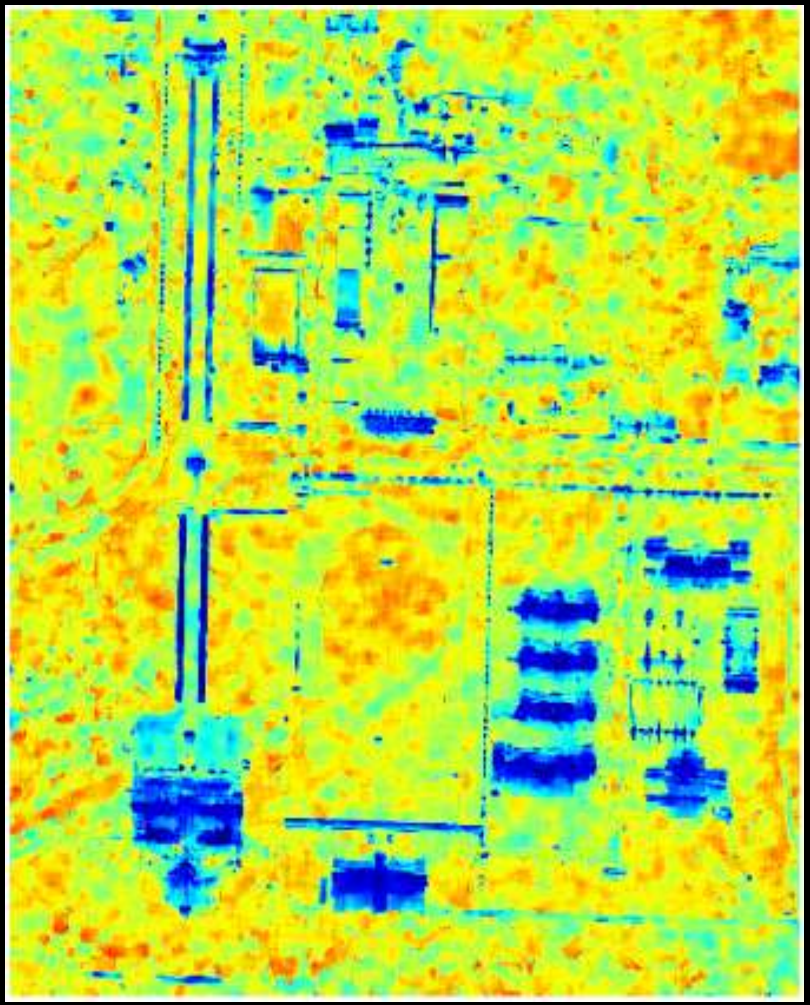

SIRV based dual-domain filter

By-product: Texture Extraction

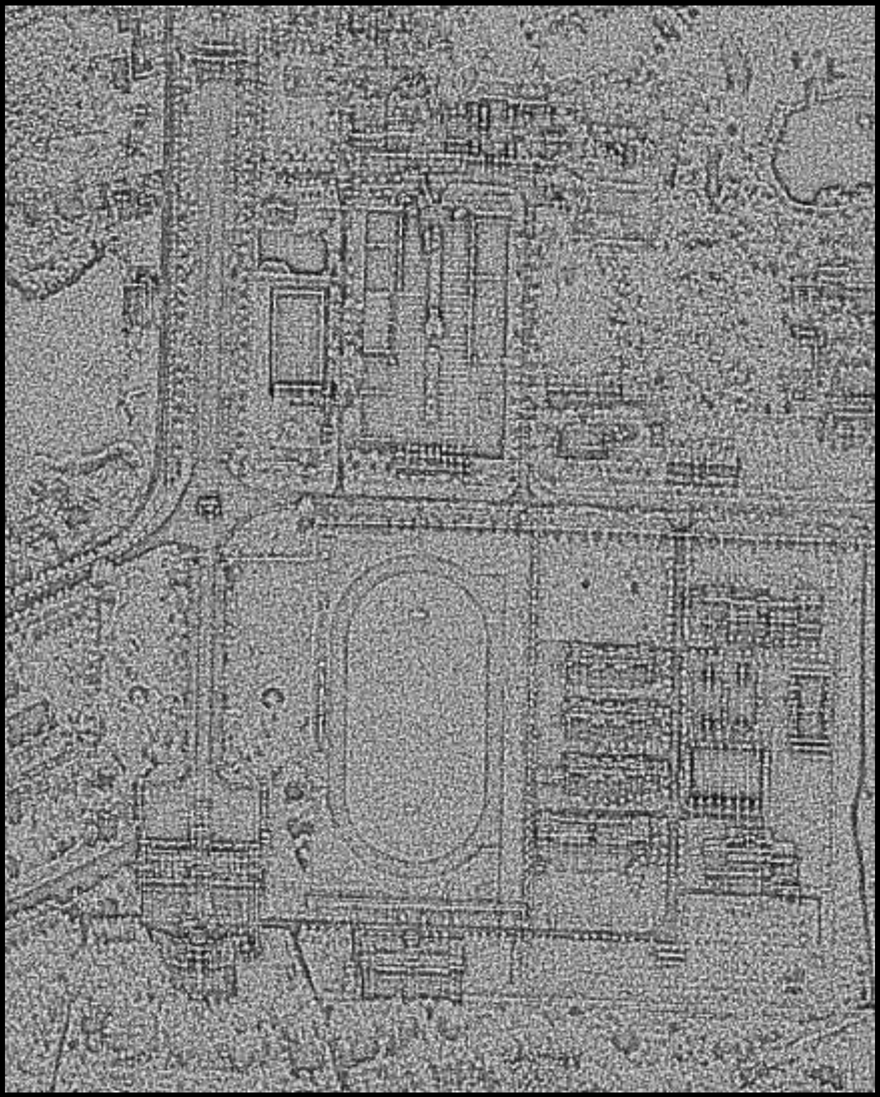

natural clutter
(before dual-domain filtering)

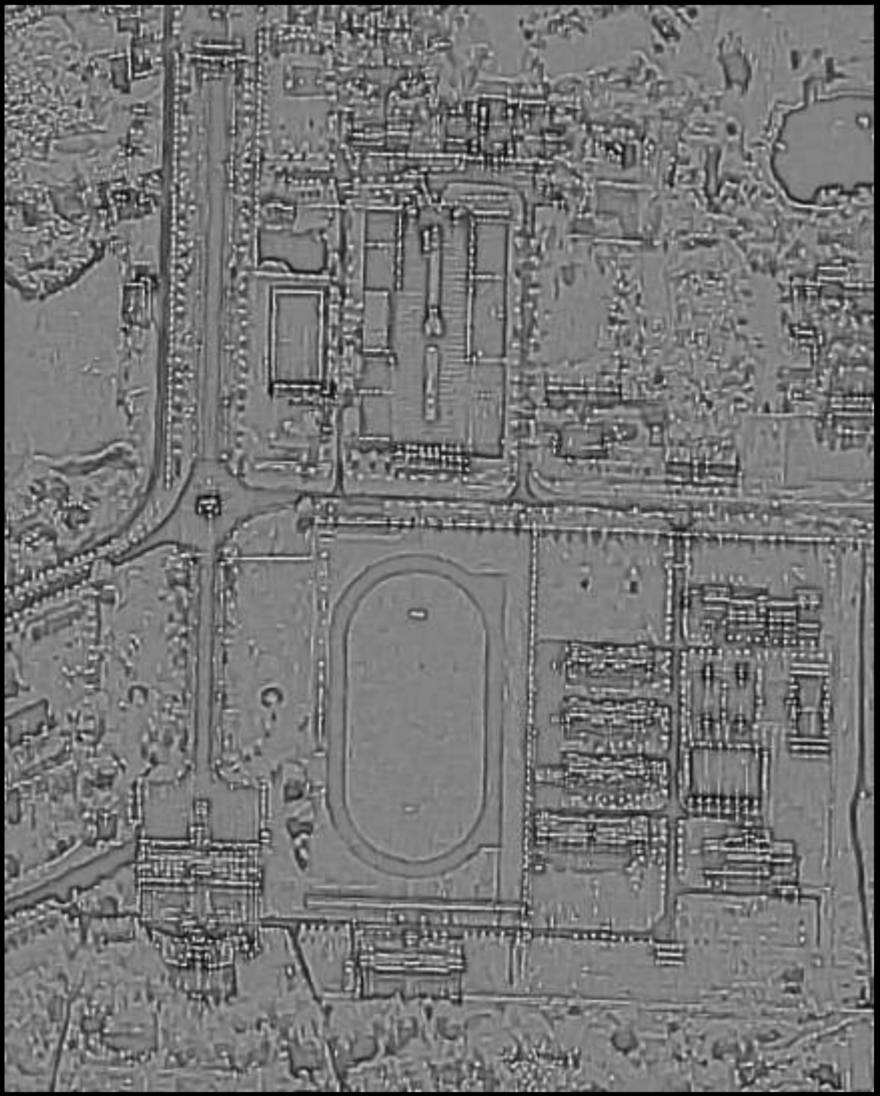

almost no natural clutter
(after dual-domain filtering)

Application: Dual-domain filter + PolSAR Classification

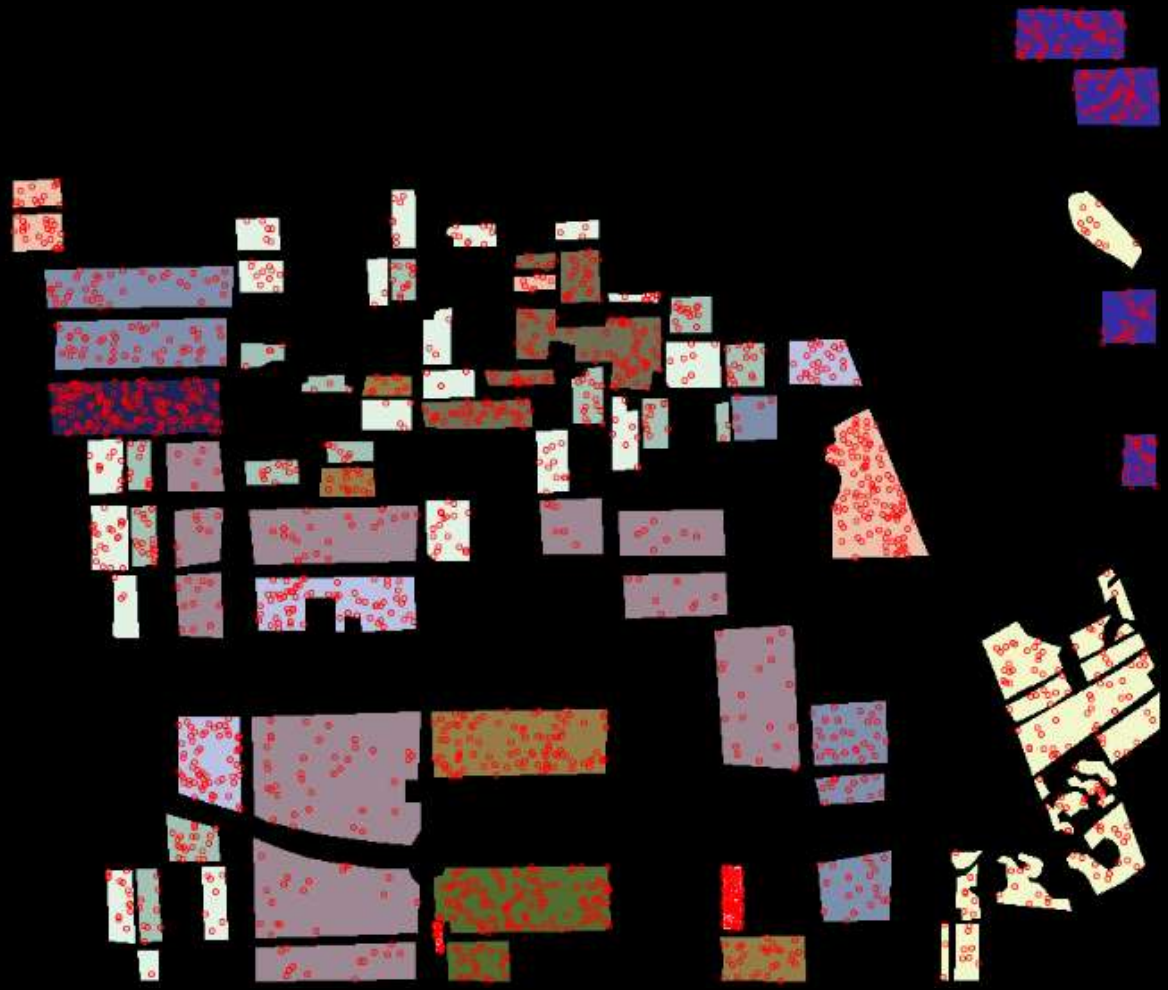

Groundtruth + Randomly select 150 training pixels for each class

Application: Dual-domain filter + PolSAR Classification

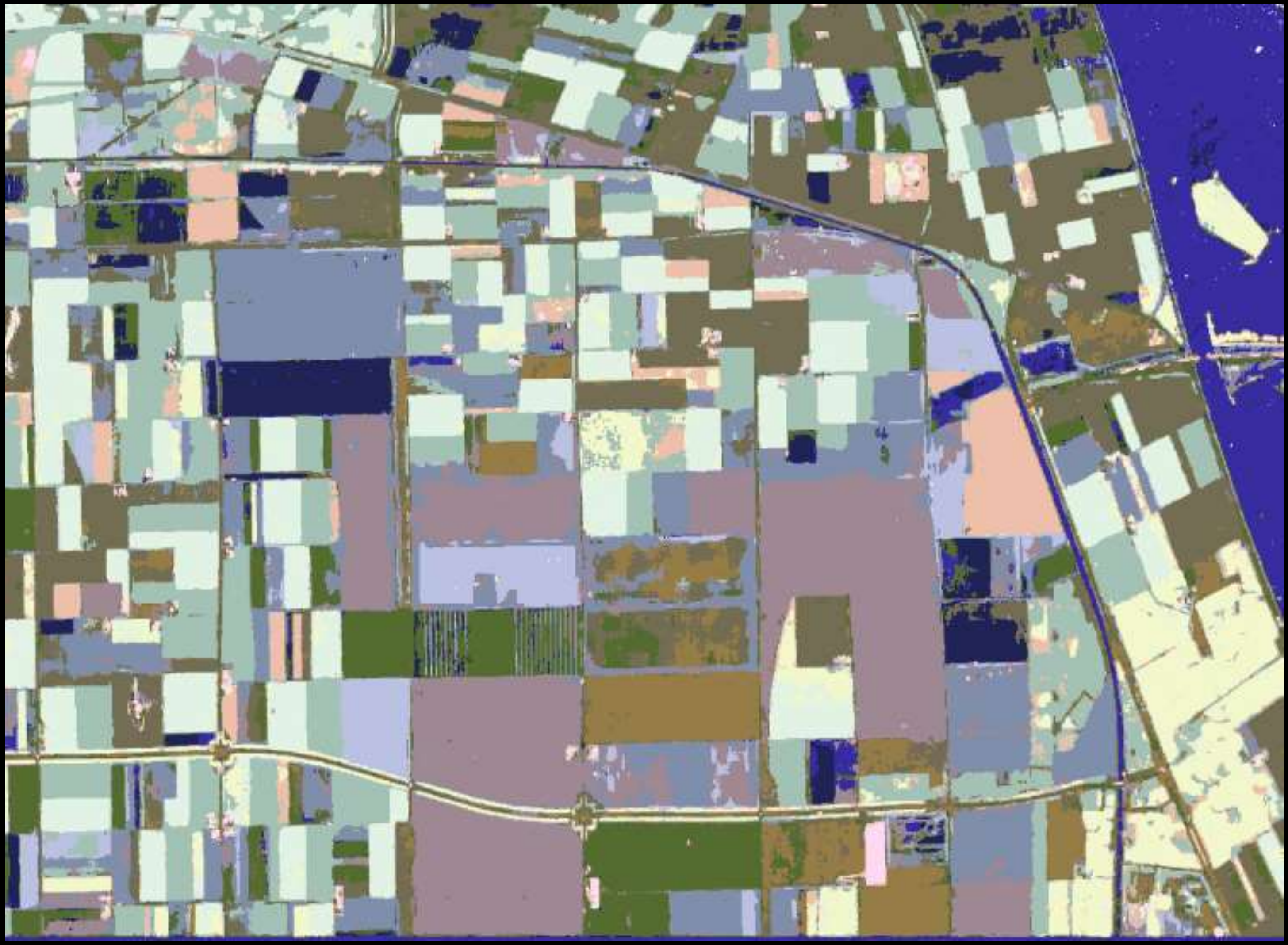

Felevoland

Accuracy: 0.9822
Kappa: 0.9795

Directly use RF without any feature extraction

Application: Dual-domain filter + PolSAR Classification

Classification details

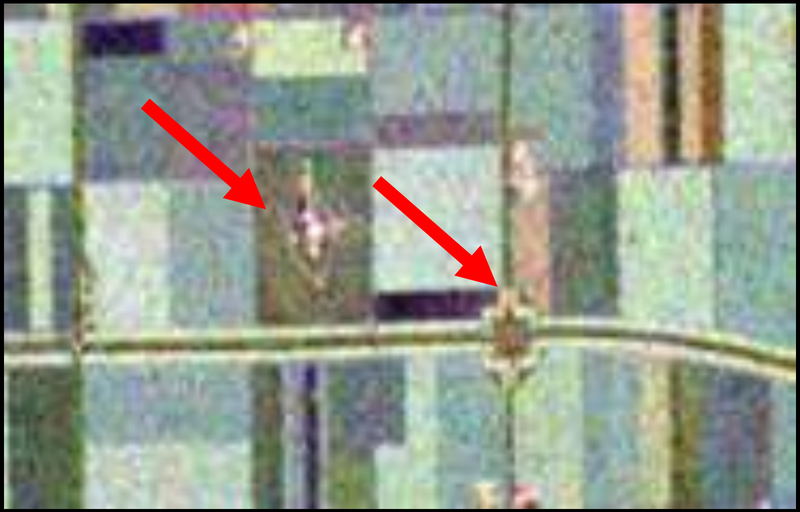

Pauli-RGB block of original PolSAR data

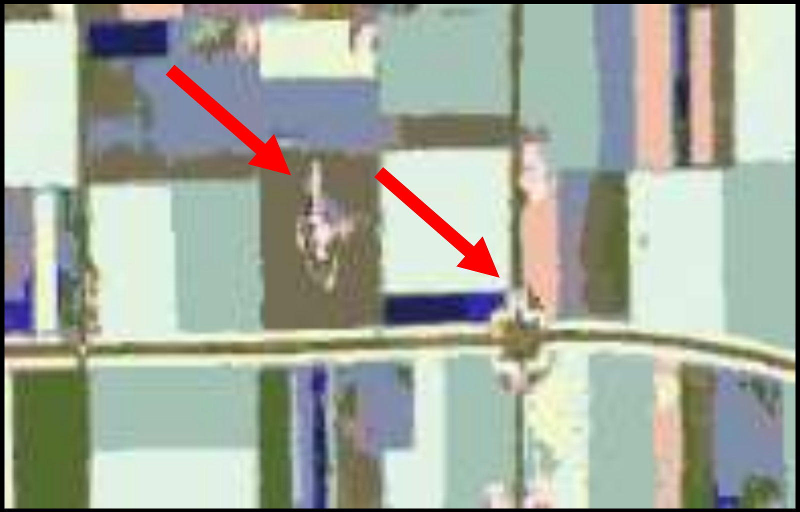

Dual-domain Filter+classifer

Boxcar 5*5+classifer

Application: Dual-domain filter + Improved FDD3

GF-3 Xi'An

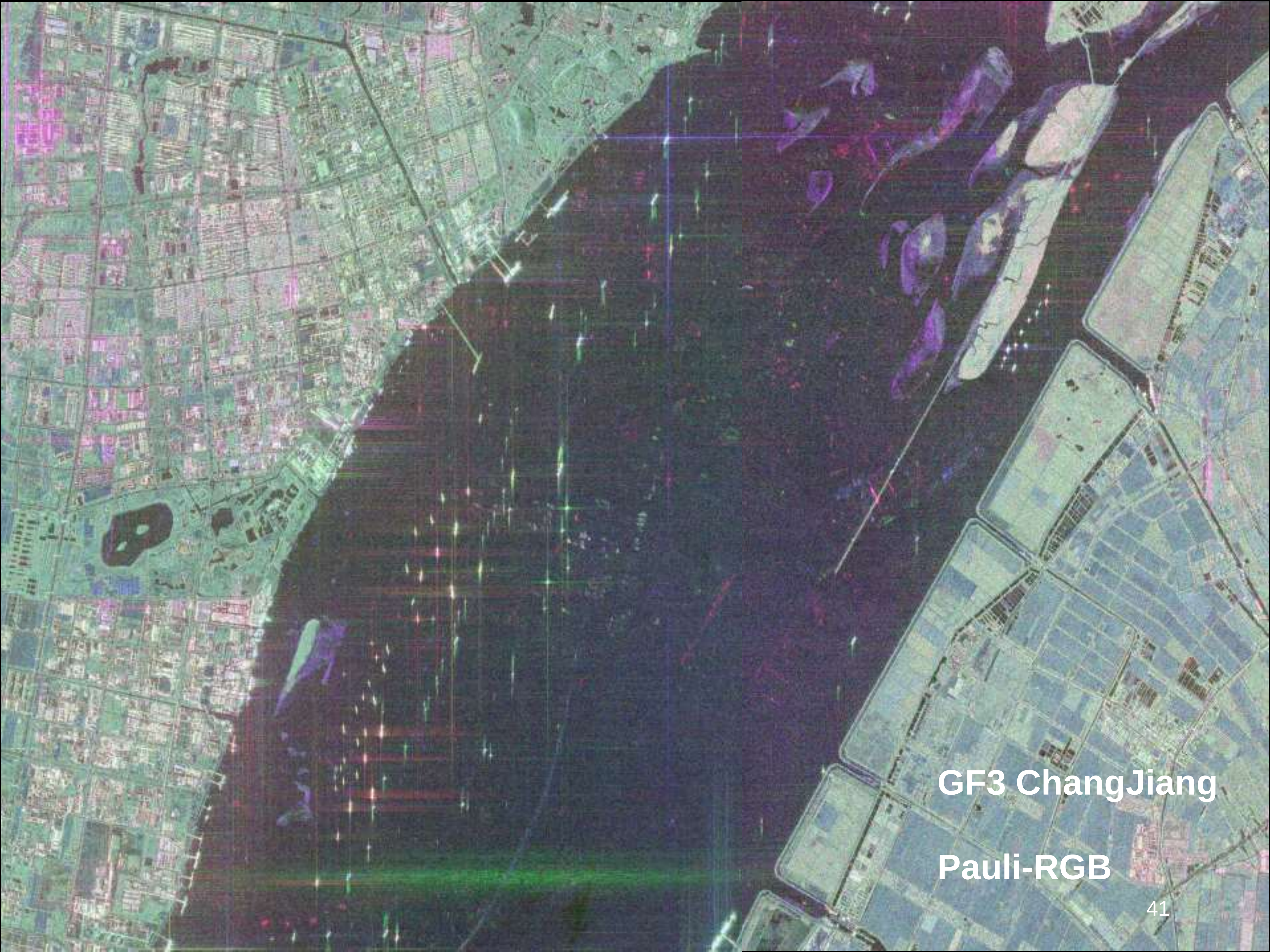
GF3 ChangJiang
Pauli-RGB

Application: Dual-domain filter + Improved FDD3

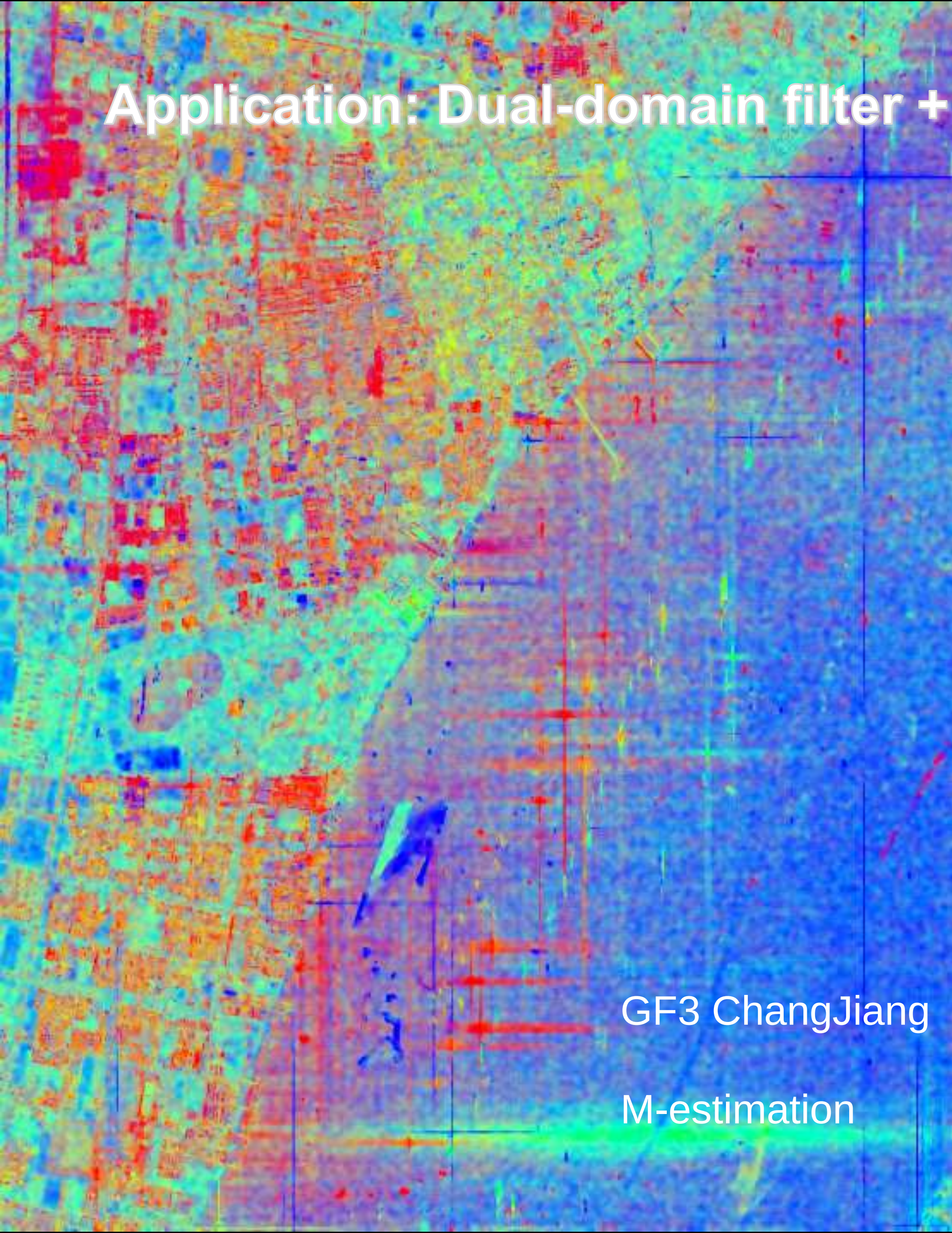

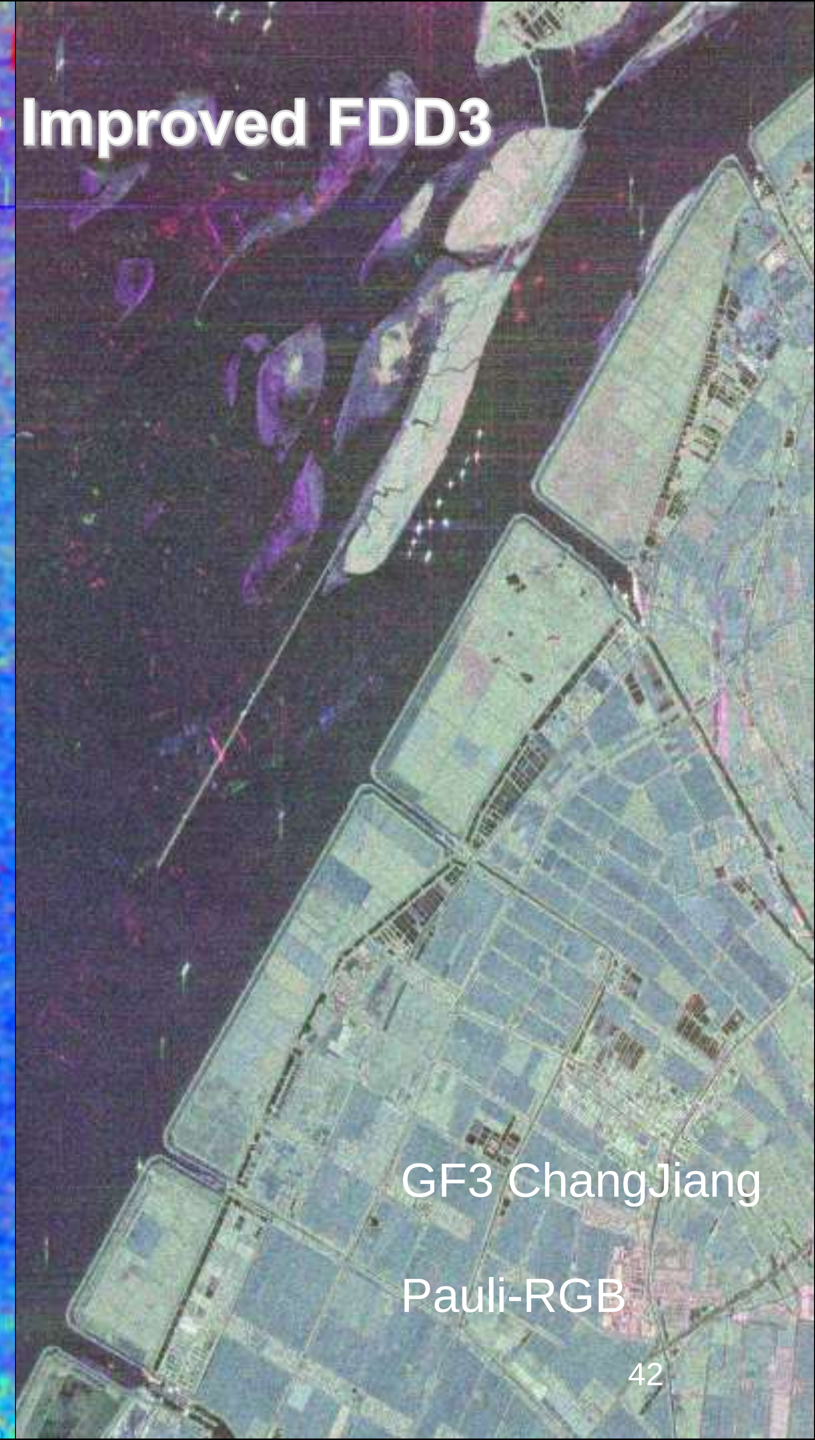

Application: Dual-domain filter + Improved FDD3

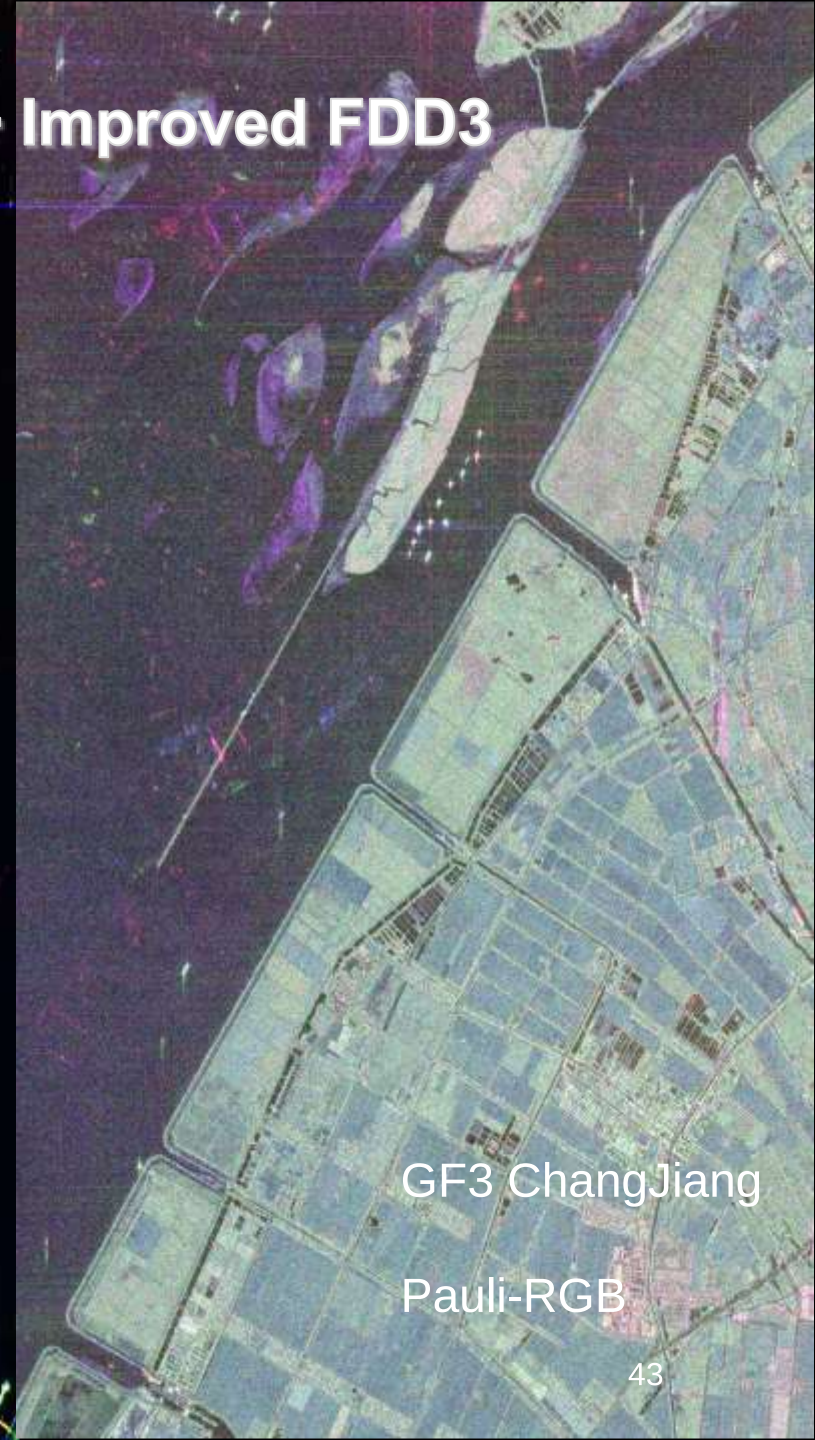

GF3 ChangJiang

Whole scene PolSAR image
No loss of resolution

SIRV-based dual-domain filter +
Improved FDD3


GF3 Shanghai
Pauli-RGB

Application: Dual-domain filter + Improved FDD3

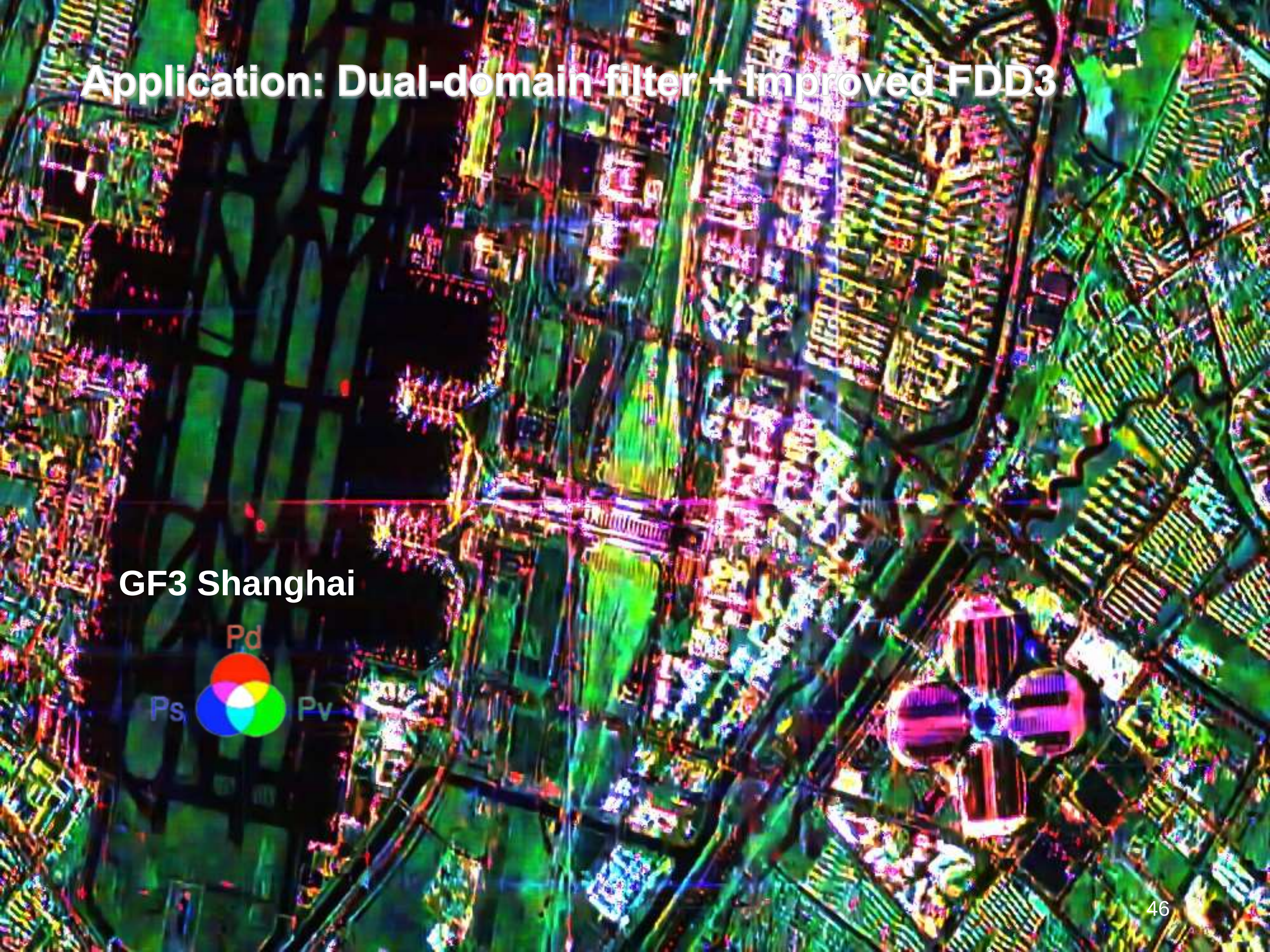

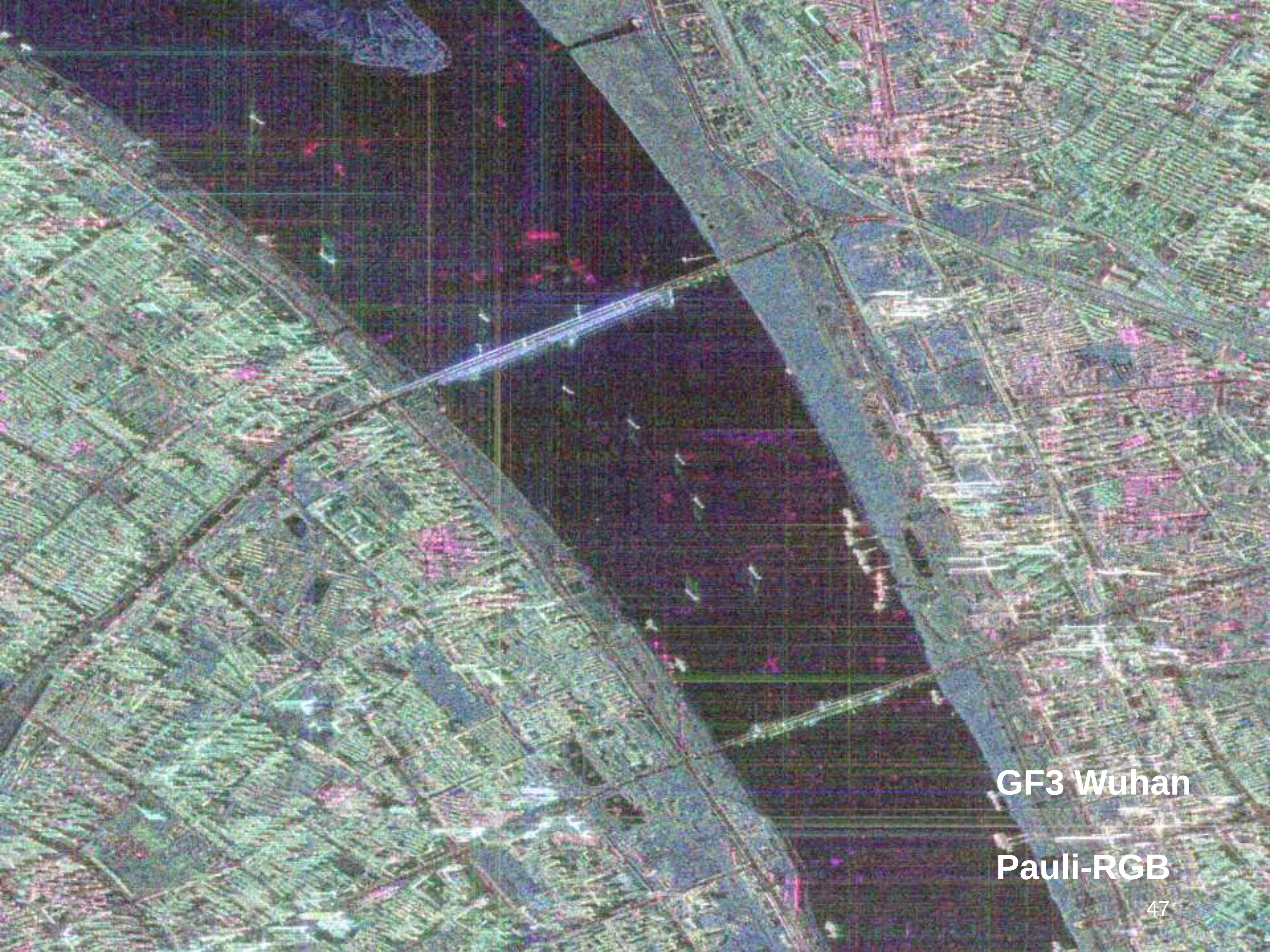
GF3 Wuhan
Pauli-RGB

Application: Dual-domain filter + Improved FDD3

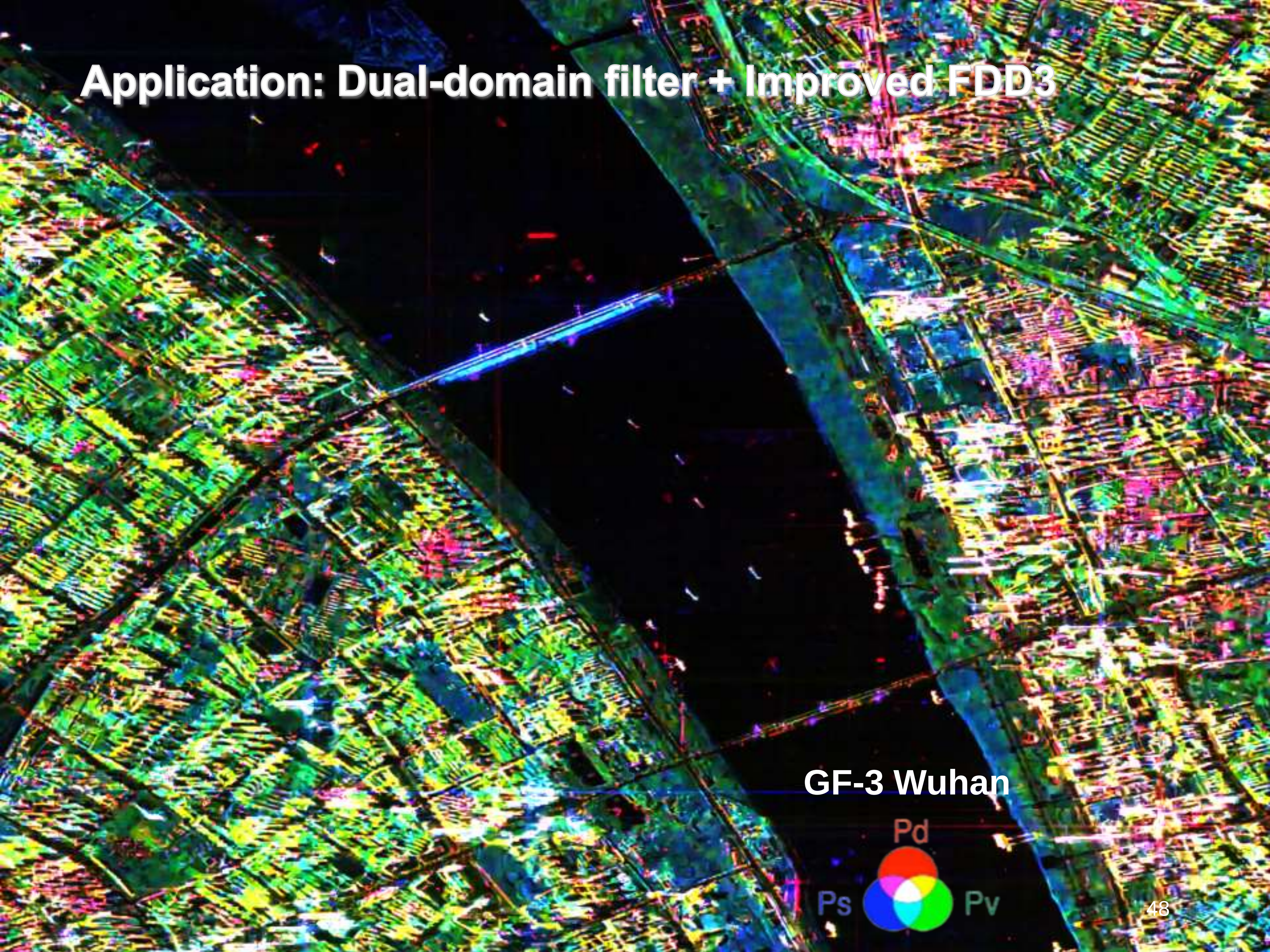

Application: Dual-domain filter + Improved FDD3

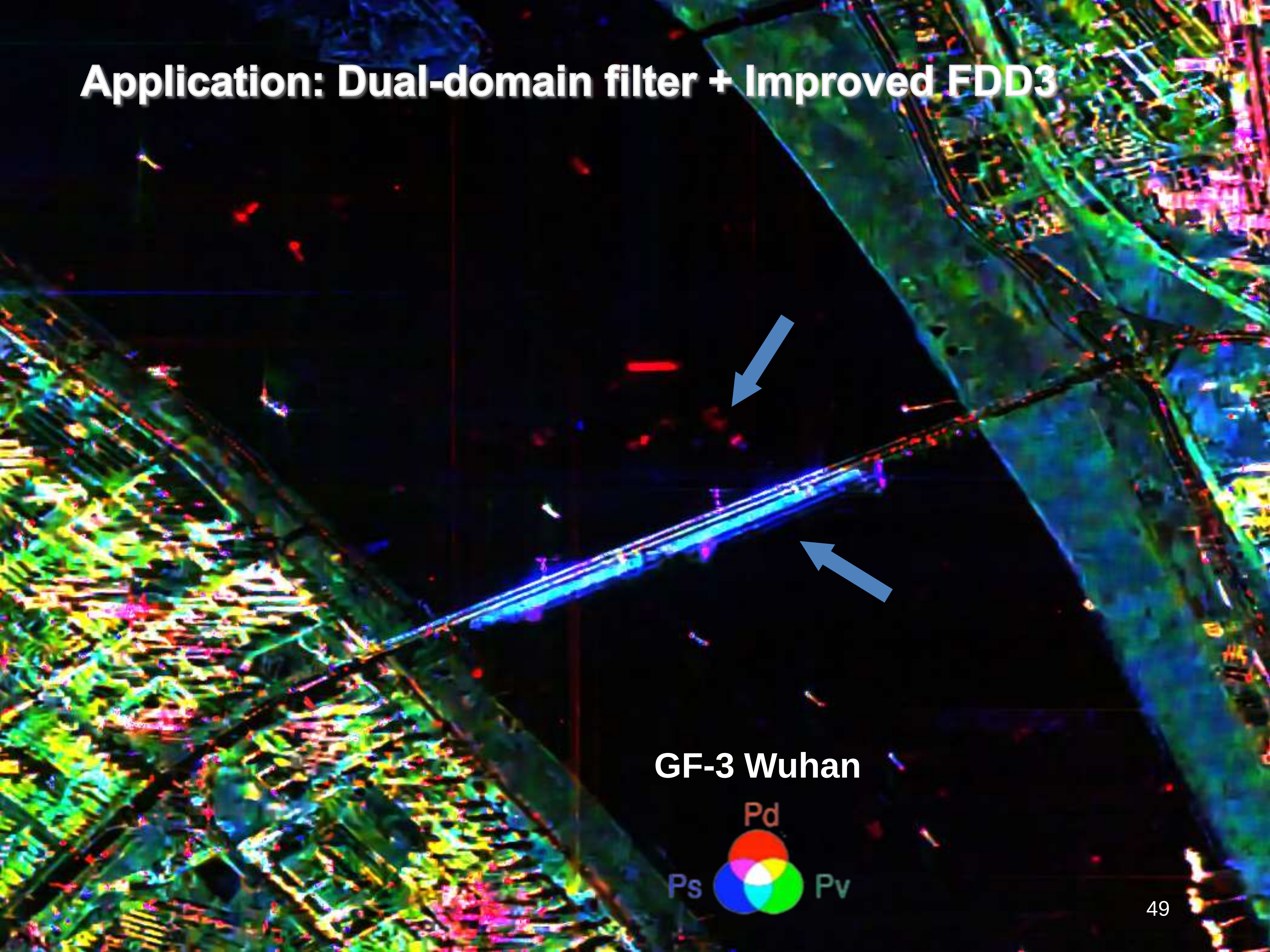

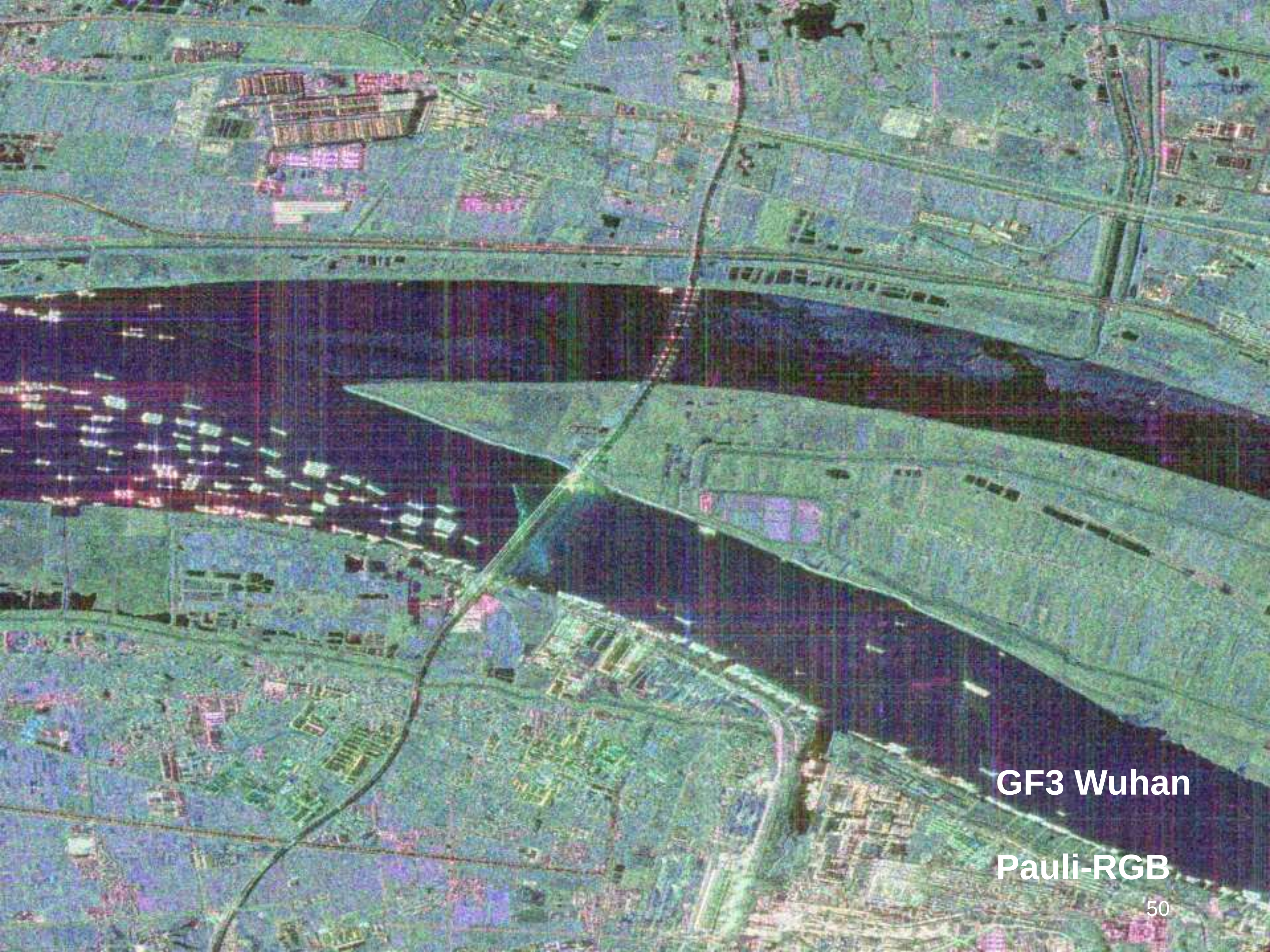
GF3 Wuhan
Pauli-RGB

Application: Dual-domain filter + Improved FDD3

Application: Dual-domain filter + Improved FDD3

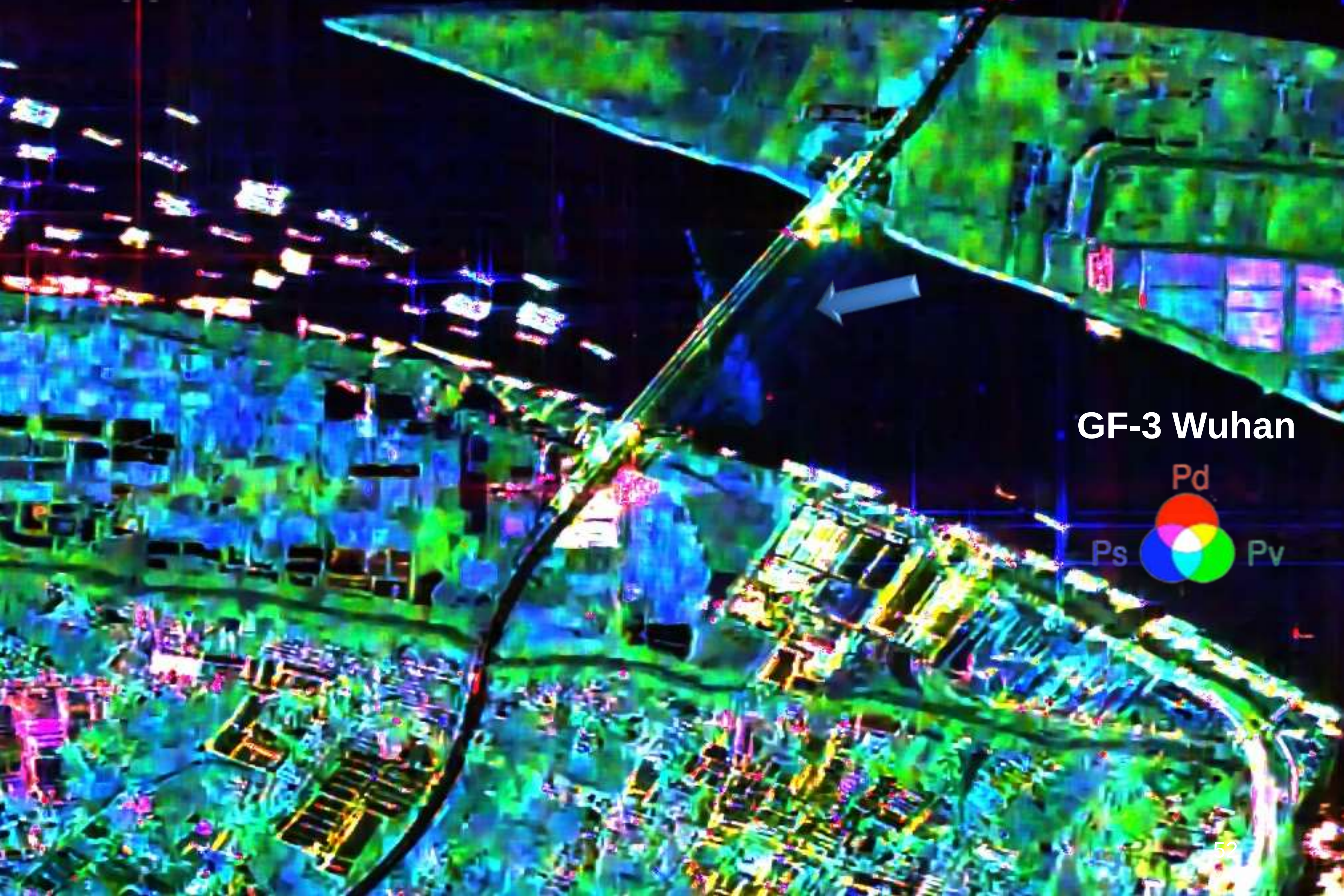

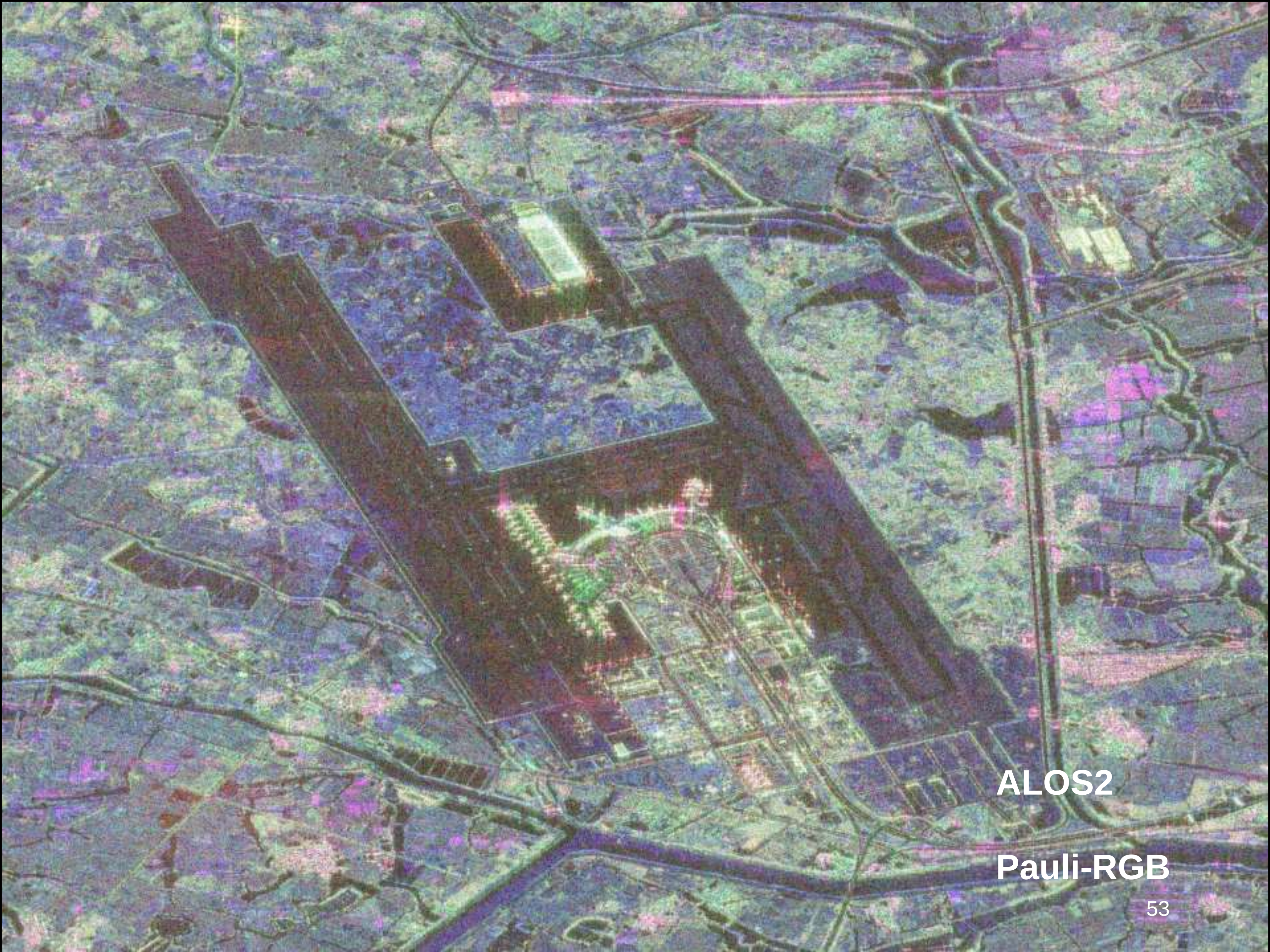
ALOS2
Pauli-RGB

Application: Dual-domain filter + Improved FDD3

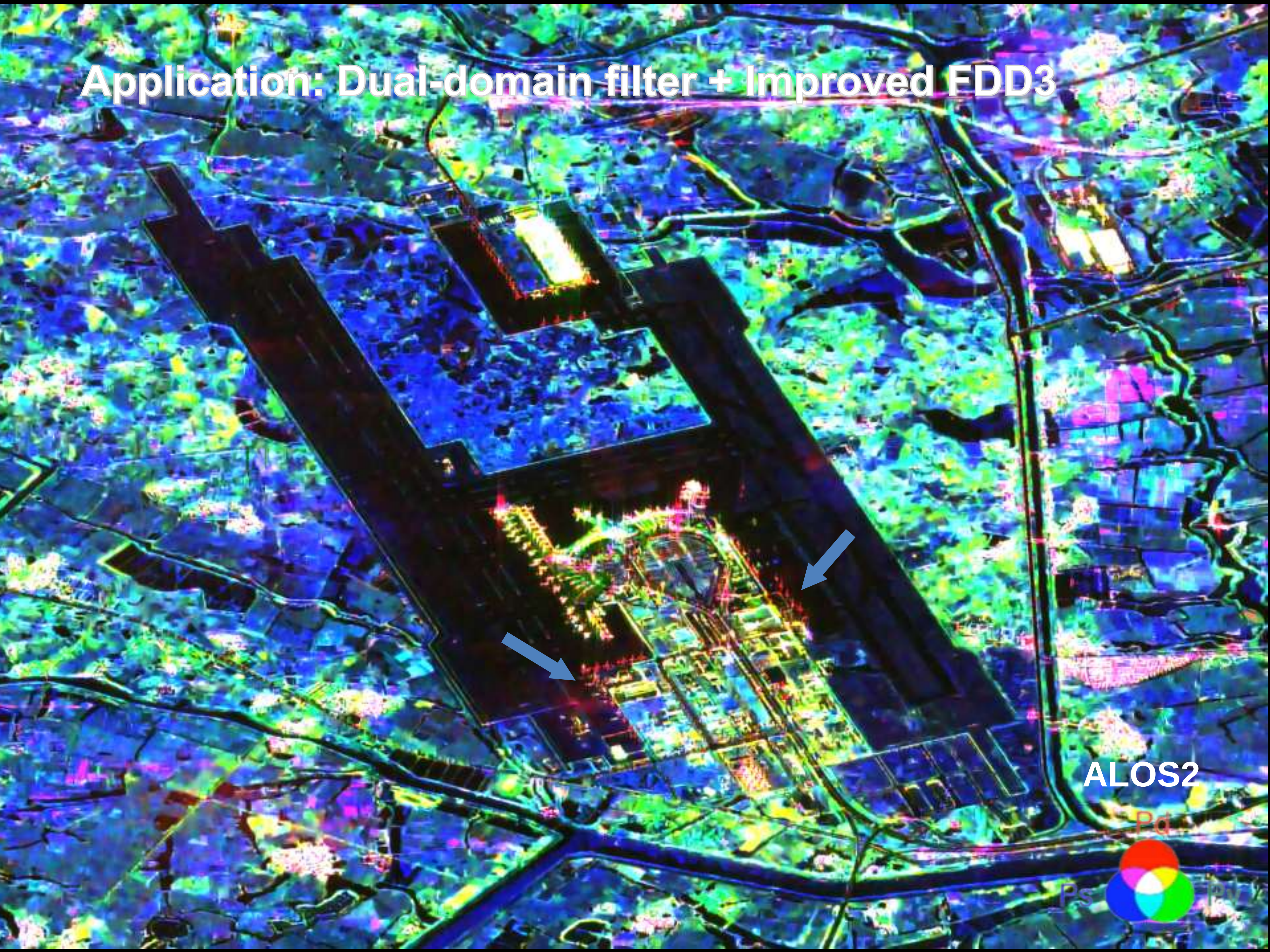

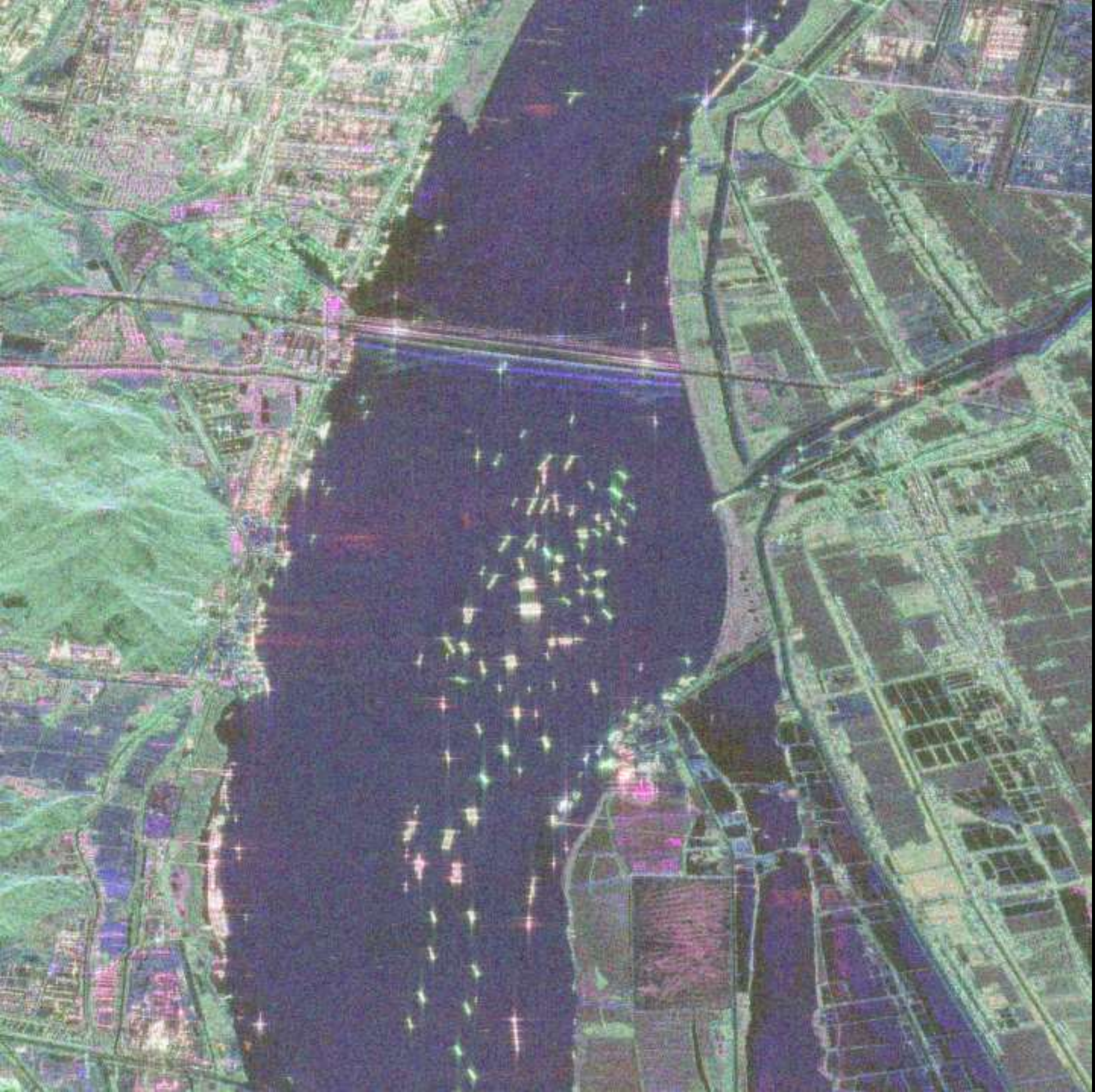

ALOS2

Pauli-RGB

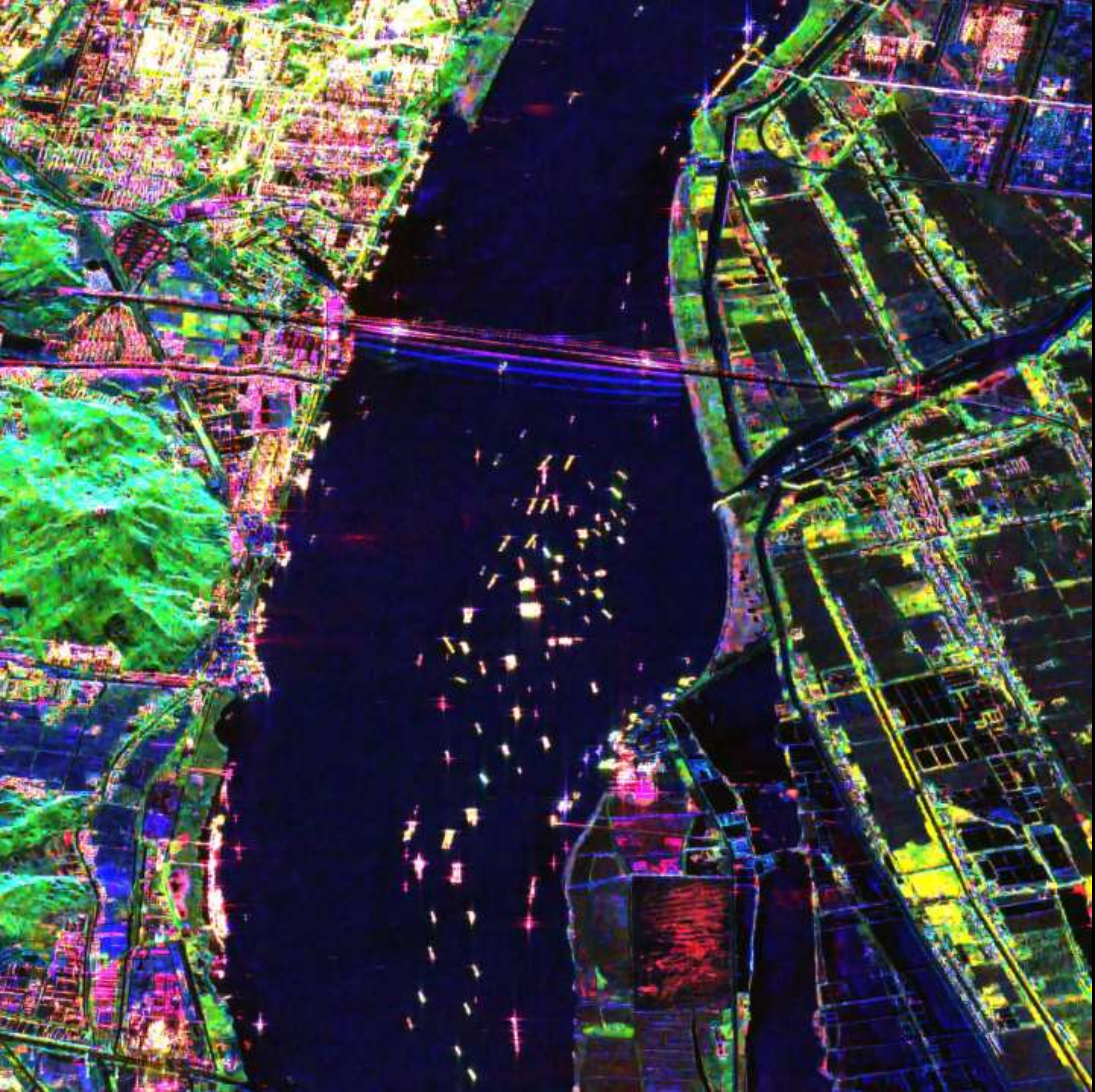

SIRV-based dual-domain filter + Improved FDD3

ALOS2

Application: Beyond PolSAR

- SIRV-based dual-domain filter for panchromatic and PolSAR image fusion

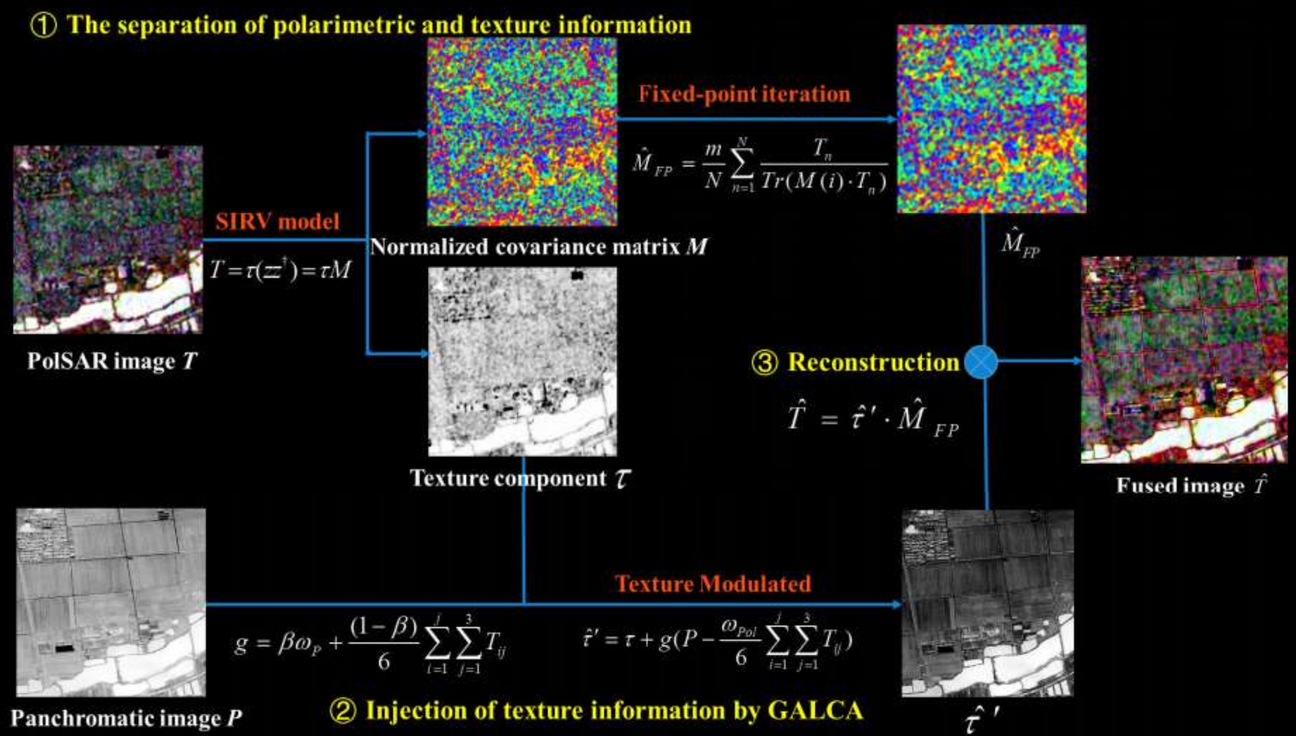

Dual-Domain Super-Resolution Image Fusion Method [*Liu. W. et al.*, 2022]

Application: Beyond PolSAR

- Clutter decomposition for the improvement of TomoSAR data quality.
  - AIRCAS Yuncheng Array-InSAR data

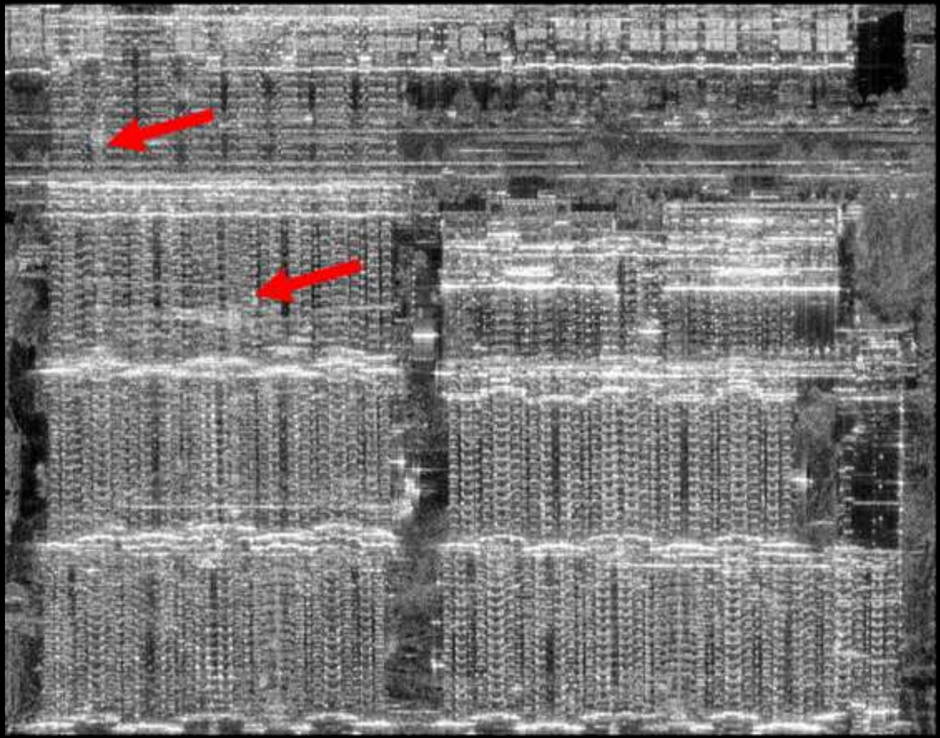

Ref: 任烨仙.稀疏阵列层析SAR相位定标与三维成像[D].复旦大学,2023.

Application: Beyond PolSAR

- Clutter decomposition for the improvement of TomoSAR data quality.
  - AIRCAS Ku Yuncheng Array-InSAR data

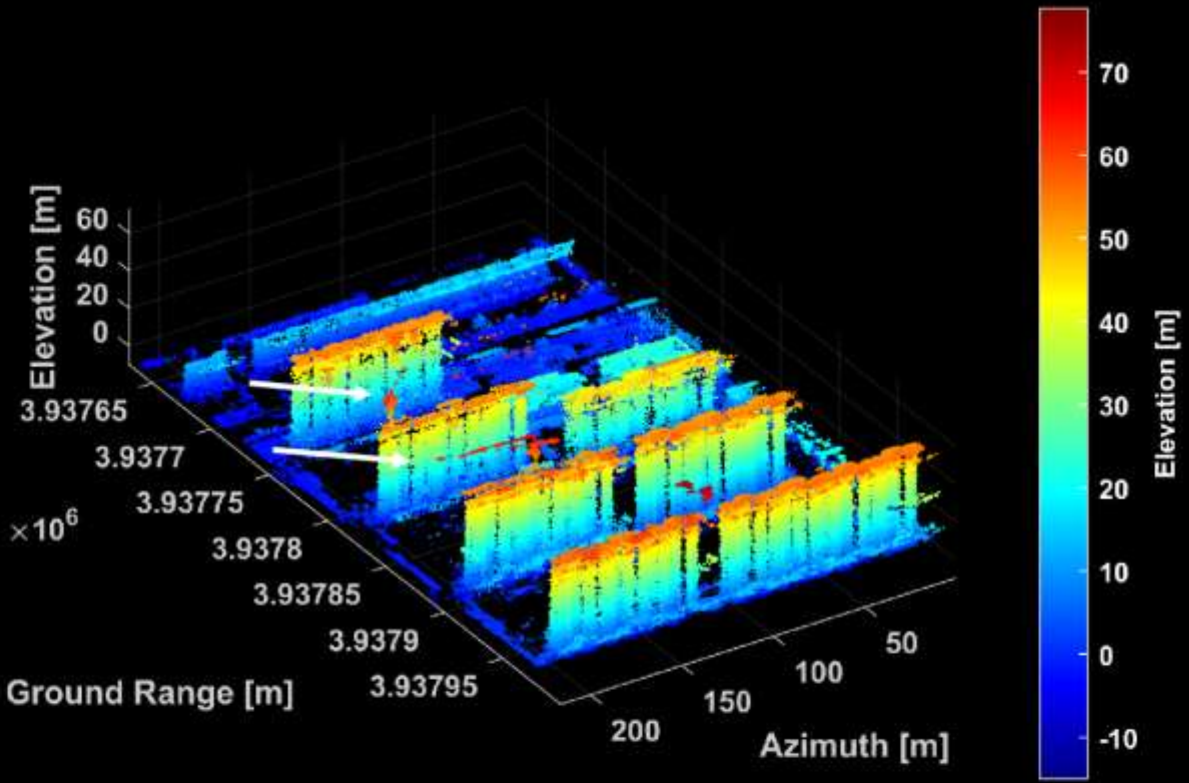

Ref: 任烨仙.稀疏阵列层析SAR相位定标与三维成像[D].复旦大学,2023.

Application: Beyond PolSAR

- Clutter decomposition for the improvement of TomoSAR data quality.
  - AIRCAS X EMei Array-InSAR data

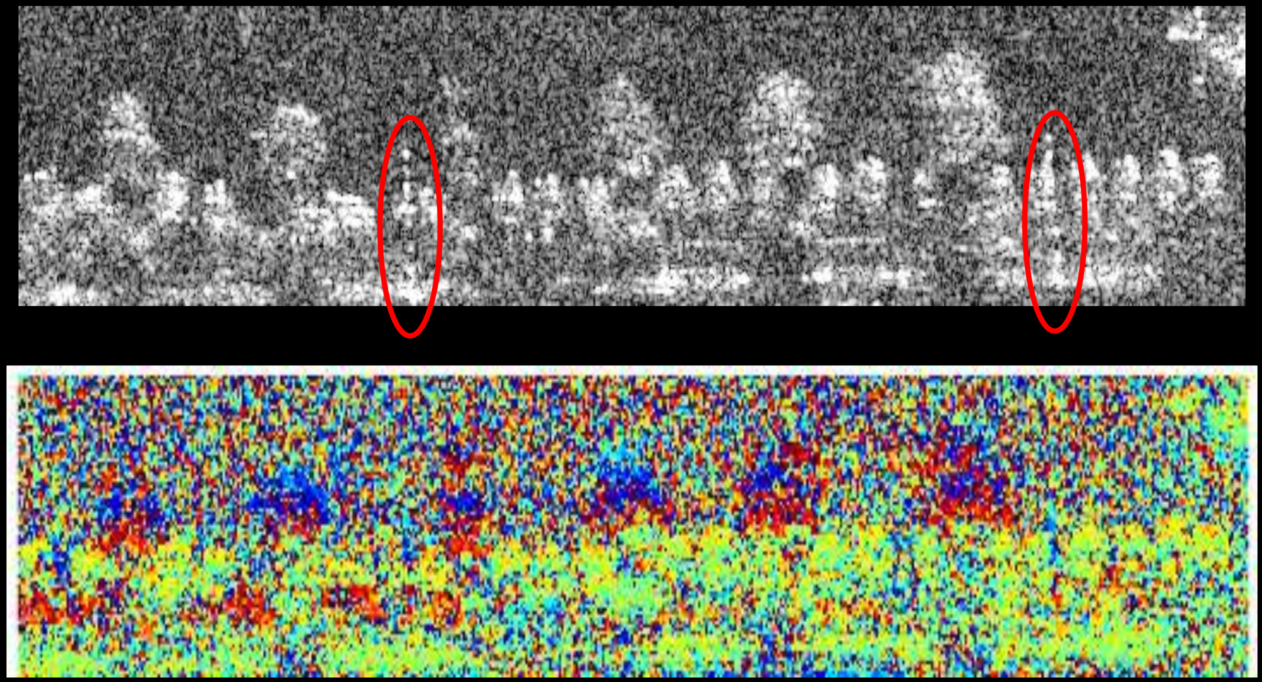

Ref: 任烨仙.稀疏阵列层析SAR相位定标与三维成像[D].复旦大学,2023.

Application: Beyond PolSAR

- Clutter decomposition for the improvement of TomoSAR data quality.
  - AIRCAS X EMei Array-InSAR data

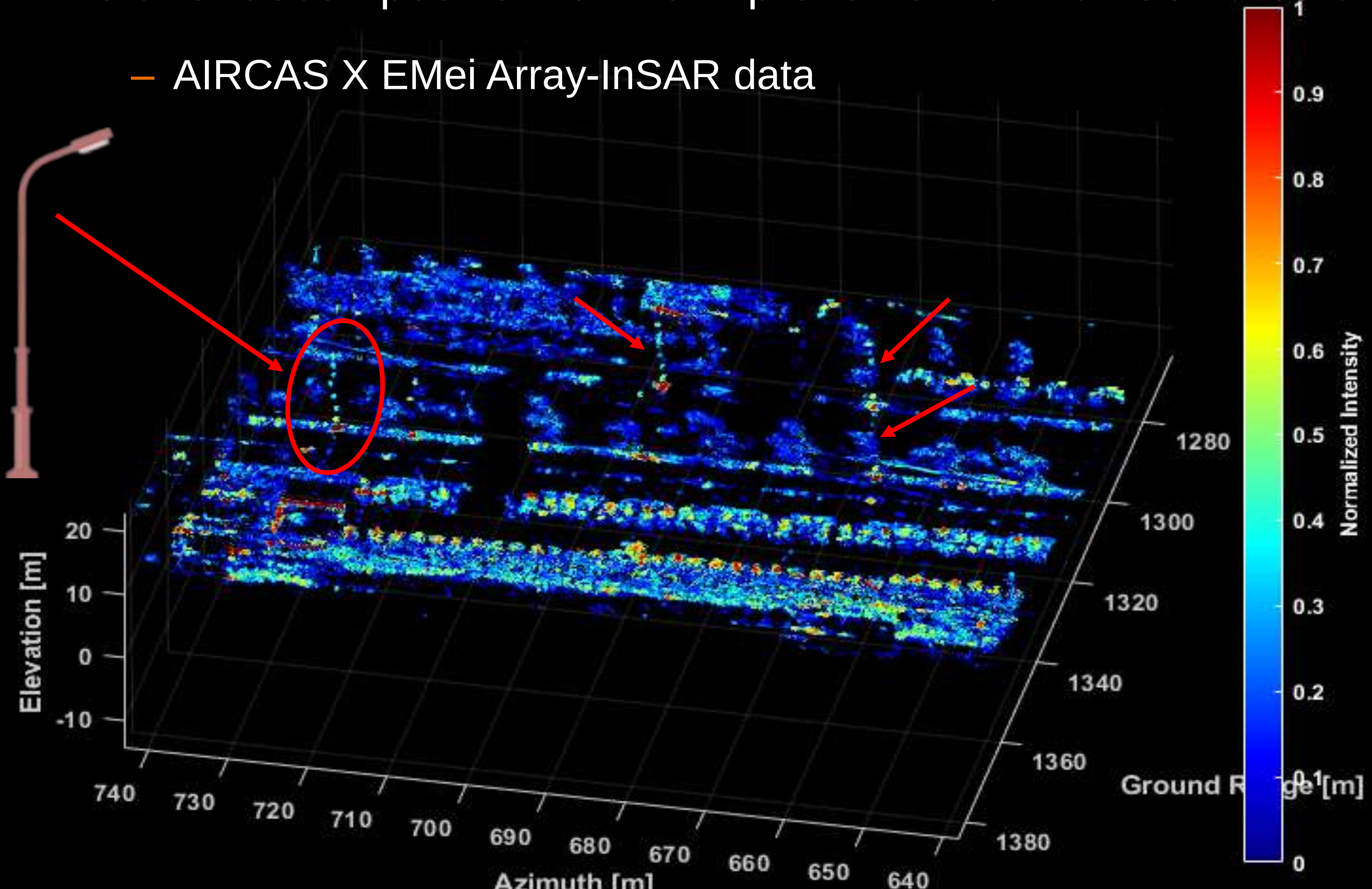

Ref: 任烨仙.稀疏阵列层析SAR相位定标与三维成像[D].复旦大学,2023.

Failure of SIRV-based dual-domain filter

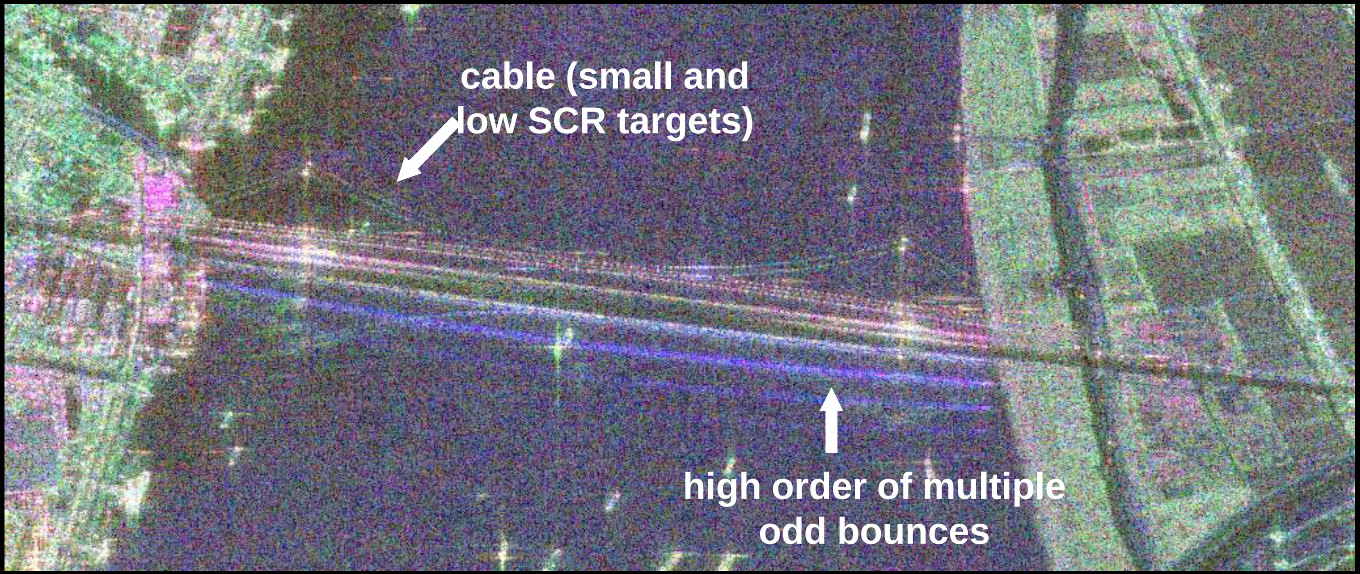

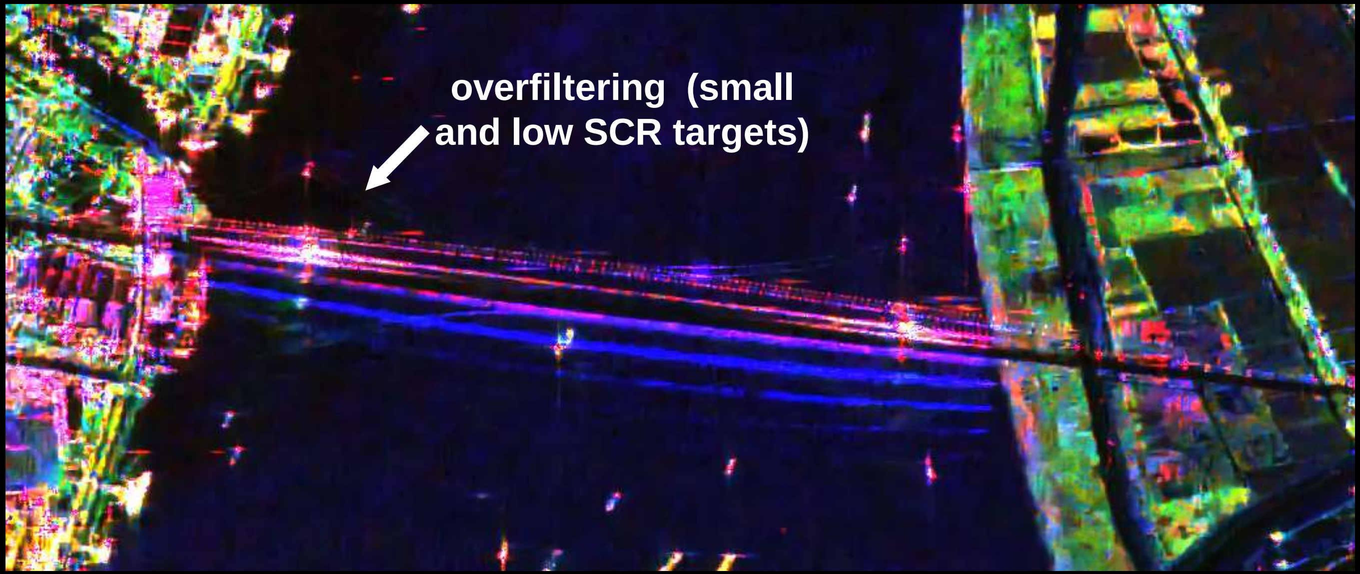

ALOS2

Failure of SIRV-based dual-domain filter

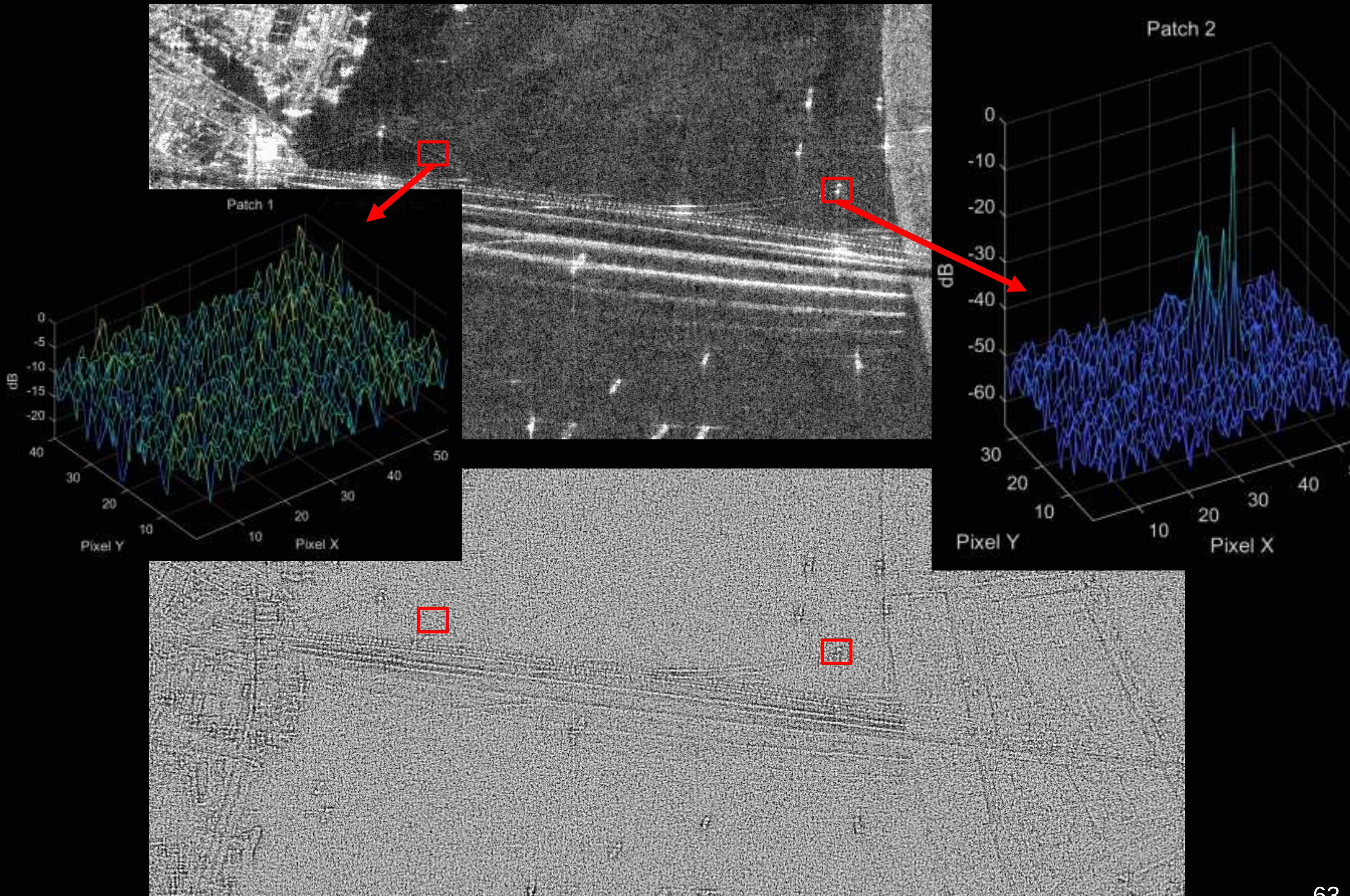

Summary

- Divide *an unsolved difficult problem into two solved sub-problems*
- SIRV-based dual-domain filter
  - Decompose heterogeneous clutter
  - Enhance signal-to-clutter ratio
  - Favour three component decomposition

Thank you!

Ref: Ren Y. , Yang J. , Zhao L., Li P., and Shi L., SIRV-based high-resolution PolSAR image speckle suppression via dual-domain filtering[J]. IEEE TGRS, 2019, 57(8): 5923-5938.